Tokyo, Japan) was then injected into the microinjection cannula. The brain was fixed with 10% formaldehyde via intracardiac infusion. Coronal sections were then made, and the injection site was localized according to the atlas (Paxinos & Watson 1996). The images were captured with an image analysis system (microscope; B×50, objective lens; 4×, OLYMPUS, Tokyo, Japan, camera; Power HAD, SONY, Tokyo, Japan, detector; MCID Elite Version 6.0, Amersham Biosciences).

Northern blotting analysis of uncoupling protein 1 mRNA in BAT

To examine the effect of ghrelin on uncoupling protein (Ucp) 1 mRNA expression in BAT, rats were killed by decapitation 3 or 6 h after i.c.v. or i.v. administration of sample and BAT was removed and stored at −80 °C.

Total RNA was extracted from rat tissues using the AGPC method. Ucp1 cDNA was amplified from BAT RNA using 5′-CCGGATCCAGGCTTCCAGTACTATTAG-3′ (sense) and 5′-CCGAATTCGCCACCCGTCATCAAGCCA-3′ (antisense) primers, which range from 310 to 547 (NCBI: BC088156). The amplified cDNA was subcloned into pGEM 3Z vector (Promega). Plasmid vector was digested by EcoRI and BamHI, and the 233 bp Ucp1 cDNA fragment was labeled using a digoxigenin (DIG) DNA labeling and detection kit (Roche Diagnostics GmbH). Twenty micrograms of total RNA was separated with 0·8% agarose gel and transferred to a positively charged nylon membrane (Roche). The membranes were fixed by u.v. cross linking and pre-hybridized in high SDS-buffered solution (7% SDS, 50% formamide, 5×SSC, 50 mM sodium phosphate, pH 7·0, 0·1% *N*-lauroylsarcosine, and 50 μg/ml yeast tRNA) at 55 °C for 2 h. DIG-labeled DNA probe was added and hybridized at 55 °C for 48–72 h. The membranes were then washed and primed with anti-DIG antibody conjugated with alkaline phosphatase. The signals were detected on Fuji Las 1000 (Fuji film, Tokyo, Japan) using CDP star detection reagent (Amersham Biosciences). Quantification of the bands was performed using an NIH image (developed by Dr Wayne Rasband; available via http://rsb.info.nih.gov), and the intensity of the bands was corrected using the density of the 18S rRNA bands. The Ucp1 mRNA level was expressed as a percentage of the control group (rats receiving saline).

RT-PCR

The tissue samples of hypothalamus, pituitary, epididymal WAT and BAT were obtained from five rats after decapitation and they were then stored at −80 °C. Total RNA was extracted from rat tissues using AGPC method. To avoid false positive results caused by DNA contamination, a DNase treatment for 60 min at 37 °C using RNase-free DNase (Takara, Shiga, Japan) was done. First strand cDNA was synthesized using 1 μg of denatured total RNA under conditions of 42 °C for 30 min, 99 °C for 5 min, and 5 °C for 5 min using a RT-PCR kit (Takara). PCR was carried out under conditions of denaturation at 94 °C for 10 s, annealing at 55 °C for 5 s, and extension at 72 °C for 30 s for 45 cycles, using specific primers for rat GHS-R1a (sense: 5′-ccagaaccacaagcagacagtga-3′; and antisense: 5′-gatggcagcgctgaggtagaa-3′), rat GHRH (5′-actctgggtgttctttgtgc-3′; and antisense: 5′-atcttt gttcctggttcctc-3′), rat GH (sense: 5′-ggatccatggctgcagactctcagactcc-3′; and antisense: 5′-ctcgagctagaaagcacagctgctttccg-3′), rat Ucp1 (sense: 5′-ccggatccaggcttccagtactattag-3′; and antisense: 5′-ccgaattcgccacccgtcatcaagcca-3′), rat leptin (sense: 5′-acggaggaaaatgtgctggag-3′; and antisense: 5′-ggtgacaatggtcttgatgaggg-3′), and rat GAPDH (sense: 5′-ggcacagtcaaggctgagaatg-3′; and antisense: 5′-atggtggtgaagacgccagta-3′). After amplification, the PCR products were subjected to 2·2% agarose gel electrophoresis, stained with 0·5 mg/μl ethidium bromide, and were then visualized under u.v. illumination.

Data analysis

All results are expressed as mean±S.E.M. The data were subjected to two- or three-way repeated-measures ANOVA with ghrelin injection, surgical operation, and time as factors. The data of basal noradrenaline release in sham-operated rats and vagotomized rats and Ucp1 expression in BAT were subjected to one-way ANOVA. Subsequently, Fisher's PLSD test for multiple comparisons was used. P values $<0·05$ were considered statistically significant.

Results

Typical histological sections indicating the location of the probes inserted into the PVN or ARC are shown in Fig. 1. Only data obtained from rats in which the tip of the injection needle was inserted into the PVN or ARC were used for the statistical analysis. The data from rats in which the tip of the injection needle was not inserted into the PVN or ARC were shown as misplacement controls in Fig. 2A.

Inhibitory effect of i.c.v. ghrelin on noradrenaline release in BAT

The effect of i.c.v. administration of ghrelin at a dose of 50 or 500 pmol on noradrenaline release in BAT is shown in Fig. 3A. There was a significant interaction between ghrelin injection and time ($F_{16,72}=3·14$; $P<0·005$). Further analysis revealed that i.c.v. administration of ghrelin at a dose of 500 pmol but not 50 pmol significantly suppressed noradrenaline release in BAT dialysates 0–20 and 20–40 min after injection ($P<0·05$). The effect of i.c.v. administration of des-acyl ghrelin at a dose of 500 pmol on noradrenaline release in BAT is shown in Fig. 3B. Des-acyl ghrelin did not affect noradrenaline release in BAT.

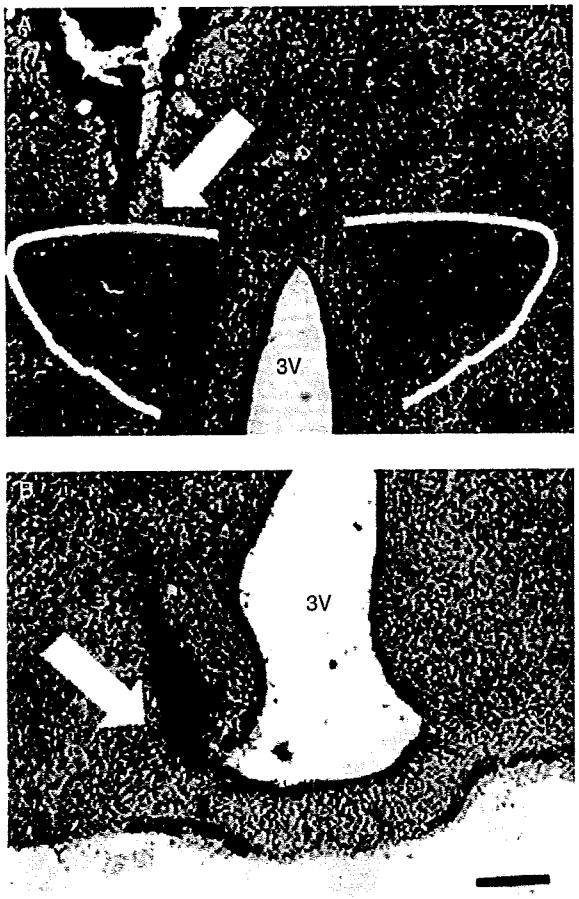

Figure 1 Histological sections showing the location (arrow) of the microinjection needle inserted into the PVN (A) and ARC (B). Nissl staining was performed. 3V, 3rd ventricle. Scale bars, 200 μm.

Inhibitory effect of ghrelin microinjected into PVN and ARC on noradrenaline release in BAT

The total number of rats used for microinjection study into the PVN was 15, and the number of rats in which ghrelin or saline was misplaced was six. The total number of rats used for microinjection study into the ARC was 16, and the number of rats in which ghrelin or saline was misplaced was seven. The effect of microinjection of ghrelin into the PVN at a dose of 50 pmol on noradrenaline release in BAT is shown in Fig. 2B. There was a significant interaction between ghrelin microinjection and time ($F_{8,\ 56}=2{\cdot}51$; $P<0{\cdot}03$). Further analysis revealed that ghrelin microinjected into the PVN significantly suppressed noradrenaline release in BAT dialysate 0–20 min after the microinjection ($P<0{\cdot}05$). The effect of the microinjection of ghrelin into the ARC at a dose of 50 pmol on noradrenaline release in BAT is shown in Fig. 2C. There was a significant interaction between ghrelin microinjection and time ($F_{8,\ 56}=2{\cdot}62$; $P<0{\cdot}02$). Further analysis revealed that ghrelin microinjected into the ARC significantly decreased noradrenaline release in BAT dialysate 0–20 min after the injection ($P<0{\cdot}05$). The effect of ghrelin on noradrenaline release in BAT was not detected in misplacement-controls, in which ghrelin was not microinjected into the PVN or ARC correctly.

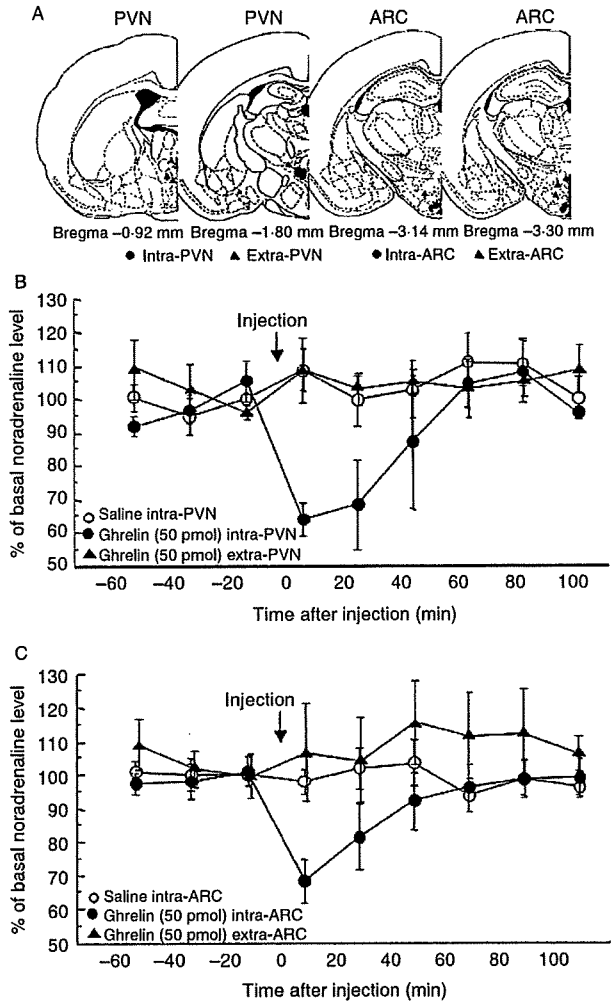

Figure 2 Effect of ghrelin microinjected into the PVN or the ARC on noradrenaline release in BAT. (A) Schematic diagram representing the sites of the tip of the microinjection needle in the PVN and ARC. Filled circles indicate the correct sites (intra-PVN or intra-ARC) and triangles indicate the misplaced sites (extra-PVN or extra-ARC) of microinjection needle tip. Stereotaxic planes were constructed according to the atlas of Paxinos & Watson (1996). (B) The effect of ghrelin microinjected into the PVN on noradrenaline release in BAT. Open circles, rats microinjected with saline into the PVN ($n=5$). Filled circles, rats microinjected with ghrelin (50 pmol) into the PVN ($n=4$) and triangles, rat microinjected with ghrelin (50 pmol) into extra-PVN regions ($n=4$). (C) The effect of ghrelin microinjected into the ARC on noradrenaline release in BAT. Open circles, rats microinjected with saline into the ARC ($n=5$). Filled circles, rats microinjected with ghrelin into the ARC (50 pmol; $n=4$) and triangles, rat microinjected with ghrelin into extra-ARC regions ($n=4$). Arrows indicate the time of sample microinjection. Values represent the mean±S.E.M. *$P<0{\cdot}05$, compared with the saline group.

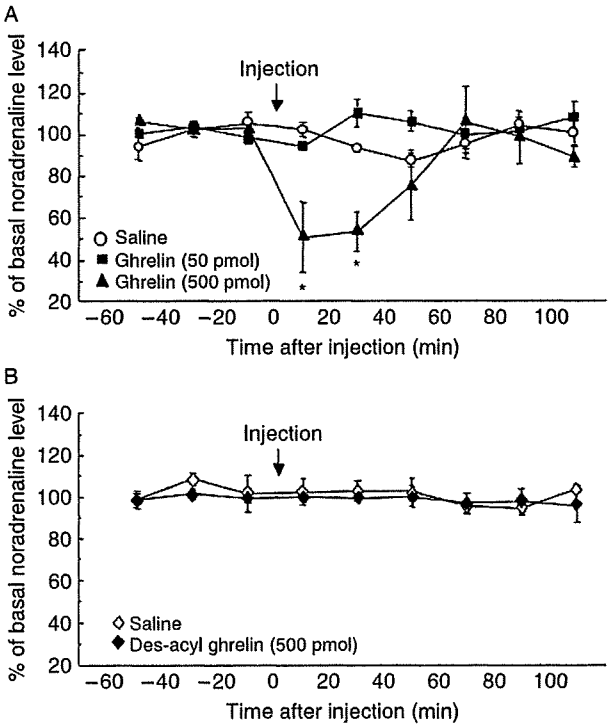

Figure 3 Effect of i.c.v. administration of ghrelin and des-acyl ghrelin on noradrenaline release in BAT. (A) I.c.v. injection of ghrelin significantly decreased noradrenaline release at a dose of 500 pmol but not 50 pmol. Circles, rats injected with saline ($n=4$). Squares, rats injected with ghrelin (50 pmol; $n=4$). Triangles, rats injected with ghrelin (500 pmol; $n=4$). (B) I.c.v. injection of des-acyl ghrelin did not influence noradrenaline release. Open diamonds, rats injected with saline ($n=4$). Filled diamonds, rats injected with des-acyl ghrelin (500 pmol; $n=4$). Arrows indicate the time of sample injection. Values represent the mean±S.E.M. *$P<0{\cdot}05$, compared with the saline group.

Inhibitory effect of i.v. ghrelin on noradrenaline release in BAT

The effects of i.v. administration of ghrelin on noradrenaline release in BAT in normal rats and vagotomized rats are shown in Fig. 4A and B respectively. There was a significant interaction between ghrelin injection and time ($F_{16,\ 96}=2{\cdot}89$; $P<0{\cdot}001$; Fig. 4A). Further analysis revealed that i.v. administration of ghrelin at a dose of 30 nmol, but not 6 nmol, significantly decreased noradrenaline release in BAT dialysate 20–40 min after injection ($P<0{\cdot}05$). There was a significant ghrelin injection×operation×time interaction ($F_{8,\ 96}=2{\cdot}12$; $P<0{\cdot}05$; Fig. 4B). The inhibitory effect of i.v. ghrelin on noradrenaline release was blocked by vagotomy. There was no significant difference in basal noradrenaline release in BAT between sham-operated and vagotomized rats (sham, 2·00±0·33 pg/20 min; vagotomized, 2·22±0·58 pg/20 min, $P=0{\cdot}78$).

The effect of i.v. administration of des-acyl ghrelin at a dose of 30 nmol on noradrenaline release in BAT is shown in Fig. 4C. Des-acyl ghrelin did not affect noradrenaline release in BAT.

Northern blotting analysis of Ucp1 mRNA in BAT

Northern blotting analysis of Ucp1 mRNA in BAT is shown in Fig. 5. There was no significant difference in Ucp1 mRNA expression in BAT between saline group and ghrelin group 3 and 6 h after their i.c.v. administration (Fig. 5A). There was also no significant difference in Ucp1 mRNA expression in BAT between saline group and ghrelin group 3 and 6 h after their i.v. administration (Fig. 5B).

RT-PCR analysis of the expression of GHS-R1a

RT-PCR analysis of GHS-R1a mRNA expression was shown in Fig. 6. There was no band of the PCR products of GHS-R1a in WAT or BAT while it was found in the hypothalamus and pituitary. As internal controls in RT-PCR, GHRH, GH, Ucp1, and leptin were used for the hypothalamus, pituitary, BAT, and WAT respectively, and their PCR products were detected.

Discussion

The present study is the first study to show that ghrelin administered centrally or peripherally inhibits noradrenaline release in BAT in conscious, free-moving rats, and the results were in accordance with a report that ghrelin administered i.c.v. inhibited the electrophysiological activity of sympathetic nerves in BAT in anesthetized rats (Yasuda *et al.* 2003). These results suggest that ghrelin inhibits the activity of BAT through the inhibition of the sympathetic nervous system. Ghrelin increases food intake when it is injected i.c.v. or i.v. (Date *et al.* 2002, Nakazato *et al.* 2001, Tamura *et al.* 2001). I.c.v. or s.c. injection of ghrelin elevates RQ in rodents, indicating an inhibitory effect of ghrelin on fat expenditure as an energy substrate (Tschöp *et al.* 2000). Furthermore, body adipose tissue is reduced in transgenic rats expressing an antisense GHS-R mRNA under the control of the promoter for tyrosine hydroxylase compared with wild rats (Shuto *et al.* 2002). Together, these results suggest that ghrelin decreases fat expenditure by inhibiting the function of brown adipocytes through the sympathetic nervous system. The i.c.v. or i.v. administration of des-acyl ghrelin, which is known not to bind to GHS-R1a, did not alter the noradrenaline release in BAT. The present study also demonstrated that GHS-R1a mRNA was not detectable in WAT or BAT of rats. These results, therefore, suggest that ghrelin modulates the activity of sympathetic nerves in BAT via GHS-R1a, and that ghrelin does not seem to act directly on brown adipocytes.

BAT plays a major role in energy expenditure and non-shivering thermogenesis in rodents. Noradrenaline released from the sympathetic nerve endings in BAT binds to β_3-adrenergic receptors on brown adipocytes and initiates intracellular breakdown of triglyceride to free fatty acid by activating hormone-sensitive lipase through an intracellular signal, cAMP (Cannon & Nedergaard 2004). Free fatty acids

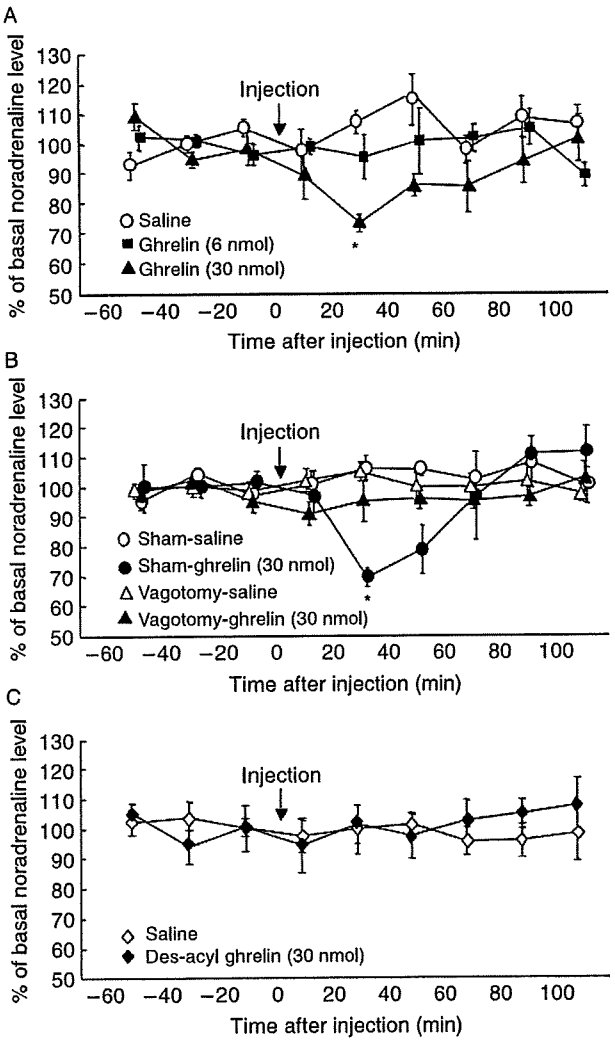

Figure 4 Effect of i.v. administration of ghrelin or des-acyl ghrelin and vagotomy on noradrenaline release in BAT. (A) The effect of i.v. administration of ghrelin on noradrenaline release in BAT. Circles, rats injected with saline ($n=4$). Squares, rats injected with ghrelin (6 nmol; $n=5$) and triangles, rats injected with ghrelin (30 nmol; $n=6$). (B) The effect of vagotomy on the suppressive action of ghrelin (30 nmol) on noradrenaline release. Open circles, sham-operated rats injected with saline ($n=4$). Filled circles, sham-operated rats injected with ghrelin (30 nmol; $n=4$). Open triangles, vagotomized rats injected with saline ($n=4$). Filled triangles, vagotomized rats injected with ghrelin (30 nmol; $n=4$). (C) The effect of i.v. injection of des-acyl ghrelin on noradrenaline release. Open diamonds, rats injected with saline ($n=4$). Filled diamonds, rats injected with des-acyl ghrelin (30 nmol; $n=4$). Arrows indicate the time of sample injection. Values represent the mean±S.E.M. *$P<0.05$, compared with the saline group.

are substrates for thermogenesis and activators of Ucp1 (Cannon & Nedergaard 2004). Ucp1 is highly expressed in brown adipocytes and is involved in thermogenesis in BAT. The i.c.v. or i.v. injection of ghrelin did not affect the expression level of Ucp1 mRNA in BAT of rats in the present study, while ghrelin inhibits Ucp1 mRNA expression in BAT in a manner independent of ghrelin-induced hyperphagia when it is chronically administered for 7 days (Tsubone *et al.* 2005, Theander-Carrillo *et al.* 2006). These findings suggest that chronic administration seems to be necessary for ghrelin to reduce the expression level of Ucp1 mRNA. It is unclear whether ghrelin administered i.c.v. influenced BAT temperature at a dose of 500 pmol in the present study since we did not measure it. However, since a study has shown that i.c.v. infusion of 1 nmol of ghrelin for 10 min causes a rapid, significant reduction of BAT temperature (Yasuda *et al.* 2003), further studies are needed to clarify how endogenous ghrelin is involved in the regulatory mechanism of BAT temperature in rats allowed access to chow *ad libitum*.

The activity of BAT is dependent on the calorie intake. Two-day fasting decreases noradrenaline turnover while cafeteria diet for 9 days increases the turnover in rats (Young *et al.* 1982). In parallel with the changes in sympathetic nerve activity, 48 h fasting decreases Ucp1 mRNA expression in rats (Champigny & Ricquier 1990) while the gene expression is elevated in mice which were exposed to high fat diet for 4 weeks (Surwit *et al.* 2000). Circulating ghrelin levels show circadian changes in rats allowed access to chow *ad libitum* (Murakami *et al.* 2002). In addition to the circadian changes, the circulating ghrelin levels increase in 3-day fasting and decrease on 30-day high fat diet (Lee *et al.* 2002). These findings therefore suggest that continuous increase or decrease of ghrelin affects the activity of BAT through the sympathetic nerves. Although it is unclear whether ghrelin influences the activities of fat storage-promoting enzymes and fat oxidation-promoting enzymes in rats, an increase in lipid droplets in BAT was found in mice which had been administered with ghrelin i.p. for 7 days (12 nmol/kg of body weight per day; Tsubone *et al.* 2005), These findings, taken together with our results, suggest that ghrelin may inhibit lipolysis in BAT.

The present study showed that ghrelin at a dose of 500 pmol but not 50 pmol inhibits noradrenaline release in BAT while previous studies have shown that ghrelin stimulates food intake and GH secretion at doses of 10 and 20 pmol respectively, when it is administered i.c.v. (Date *et al.* 2000, Nakazato *et al.* 2001). The present study also showed that ghrelin at a dose of 30 nmol but not 6 nmol inhibits noradrenaline release in BAT while other studies have shown that ghrelin stimulates food intake and GH secretion at doses of 1·5 and 1·2 nmol respectively, when it is administered i.v. (Date *et al.* 2002, Tamura *et al.* 2002). These results suggest that the threshold for ghrelin to suppress noradrenaline release in BAT may be higher than that for ghrelin to stimulate food intake or GH secretion. Another possible explanation for the results is that noradrenaline release in BAT is already suppressed by endogenous ghrelin to some extent in a tonic way, thus requiring higher doses of exogenous ghrelin for further inhibition of noradrenaline release. This seems likely as we have found that i.c.v. administration of [D-Lys^3]-GHRP6, an GHS-R antagonist, significantly increases noradrenaline release in BAT (Mano-Otagiri, unpublished observation). Furthermore,

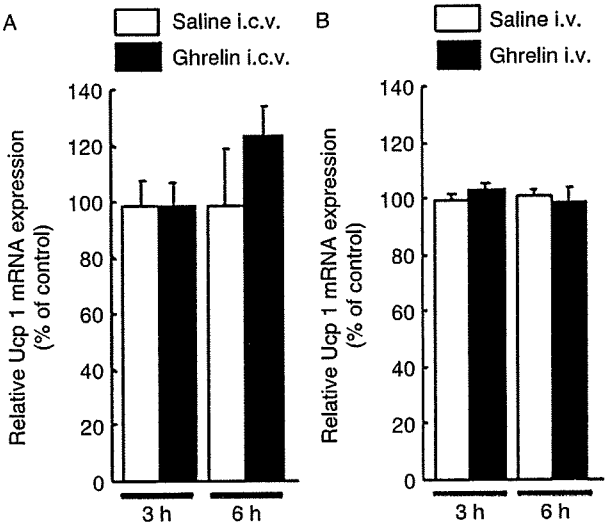

Figure 5 Effect of ghrelin on Ucp1 mRNA expression in BAT. (A) The expression of Ucp1 mRNA in BAT was not influenced by i.c.v. administration of ghrelin (500 pmol) 3 or 6 h after administration. Open bars, rats injected with saline ($n=5$). Filled bars, rats injected with ghrelin ($n=6$). (B) The expression of Ucp1 mRNA in BAT was not influenced by i.v. administration of ghrelin (30 nmol) 3 or 6 h after administration. Open bars, rats injected with saline ($n=5$). Filled bars, rats injected with ghrelin ($n=4$). Values represent the mean±S.E.M.

since plasma ghrelin concentrations rise in the afternoon and reach a peak at 1500 in rats allowed access to chow and water *ad libitum* (Murakami *et al.* 2002) and the time of ghrelin administration in the present study was around 1400–1500 when endogenous ghrelin concentrations in plasma are suggested to be high, the elevated concentrations of endogenous ghrelin might increase doses of exogenous ghrelin to further inhibit noradrenaline release in BAT.

The present study also shows that a vagotomy blocks the inhibitory effect of i.v. ghrelin on noradrenaline release. It is not likely that ghrelin could not reduce noradrenaline release further because of lowered noradrenaline release in vagotomized rats as there was no significant difference in basal noradrenaline release in BAT between sham-operated and vagotomized rats. It is therefore suggested that the vagal nerve mediates the peripheral ghrelin signal to the central nervous system to inhibit the activity of sympathetic nerves innervating BAT. Recently, it has been suggested that the afferent vagal nerve mediates the stimulatory action of peripherally administered ghrelin on food intake or GH secretion (Date *et al.* 2002), because GHS-R1a is expressed in 20% of cells of the vagal nodose ganglion (Burdyga *et al.* 2006) and the stimulatory effects of peripherally administered ghrelin on food intake and GH secretion are blocked and attenuated respectively, by vagotomy or capsaicin-induced blockade of vagal afferent signaling (Date *et al.* 2002). Peripheral ghrelin-induced food intake is also abolished by bilateral midbrain transections rostral to the nucleus solitary tract (Date *et al.* 2006). The nucleus solitary tract mediates the vagal afferent signal to the ARC through its noradrenergic projection. Therefore, the peripheral ghrelin signal to suppress the activity of BAT seems to be transmitted through the afferent vagal nerve and the nucleus solitary tract to the central sympathetic nervous system controlling BAT.

The effects of ghrelin in the PVN and ARC on noradrenaline release in BAT seem to be region-specific as ghrelin did not show the effects when it was microinjected into extra-PVN or -ARC regions. A microinjection of ghrelin into the PVN or ARC increases food intake and RQ in rats (Currie *et al.* 2005). Since the PVN and ARC express GHS-R1a (Zigman *et al.* 2006), these findings together with our present results may indicate that ghrelin directly activates GHS-R1a in the PVN and ARC and induces a suppressive effect on the sympathetic

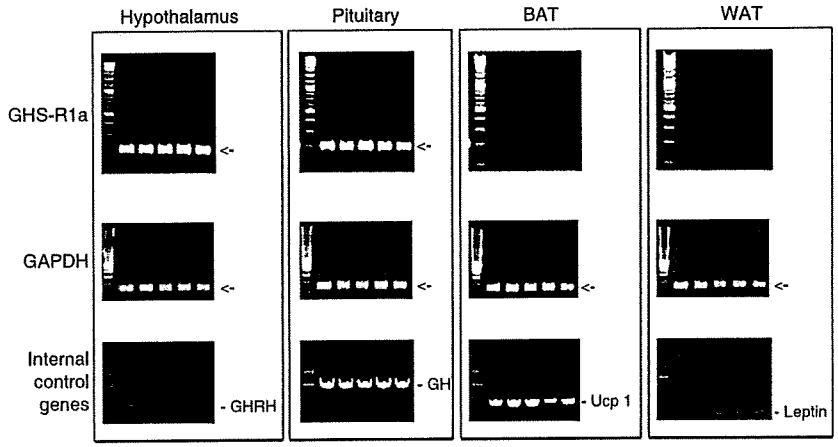

Figure 6 Expression of GHS-R1a mRNA. The band of RT-PCR product of GHS-R1a was not detected in BAT or WAT while it was detected in the hypothalamus and pituitary. The RT-PCR products of GHRH, GH, Ucp1, and leptin were found in the hypothalamus, pituitary, BAT, and WAT respectively, as internal controls.

nervous system innervating BAT. After injection of the neurotropic virus pseudorabies into BAT, infected neurons were present in the PVN, lateral hypothalamus, perifornical region, and retrochiasmatic nucleus (Oldfield *et al.* 2002). A slightly longer survival time for virus-infected neurons appeared in the ARC and dorsomedial hypothalamus (Oldfield *et al.* 2002). Another report indicated that raphe pallidus and the PVN were the main areas containing sympathetic premotor neurons activated by cold exposure (Cano *et al.* 2003). Since most of these hypothalamic areas express GHS-R1a, it seems that some of these areas are involved in the regulatory mechanism of sympathetic nervous system activity by ghrelin. Although it is unclear if microinjection of ghrelin into the lateral hypothalamus, dorsomedial nucleus, perifornical region, retrochiasmatic nucleus, and raphe pallidus suppresses noradrenaline release in BAT, our results indicate that at least the PVN and ARC may control sympathetic outflow to BAT through activation of GHS-R1a.

In summary, we found that centrally or peripherally administered ghrelin inhibits noradrenaline release in BAT and that a vagotomy blocks the inhibitory effect of peripheral ghrelin on BAT. These results suggest that central and peripheral ghrelin/GHS-R1a may play an important role in the regulatory mechanism of energy metabolism by suppressing the sympathetic nervous system innervating brown adipocytes and that the GHS-R1a expressed in the vagal nerve may be involved in the signal transduction of peripheral ghrelin to control the function of brown adipocytes. It is also suggested that the PVN and ARC may be the sites of ghrelin action in the central nervous system to inhibit the sympathetic outflow controlling brown adipocytes.

Declaration of interest

The authors declare that there are no conflicts of interest that would prejudice the impartiality of the work reported herein.

Funding

This study was supported in part by Health and Labor Sciences Research Grants from the Ministry of Health, Labor and Welfare of Japan, Grants-in-Aid for Scientific Research from the Ministry of Education, Culture, Sports, Science and Technology of Japan, and a grant from the Foundation for Growth Science.

Author contribution statement

Asuka Mano-Otagiri designed the study and wrote the protocol under the instruction of Tamotsu Shibasaki. Hisayuki Ohata, Azusa Iwasaki-Sekino and Takahiro Nemoto contributed to perform the experiments in parts of microinjection, i.v. catheterization and analysis of Ucp1 and GHS-R1a mRNA respectively.

Acknowledgements

We thank Ms M Iketani for her technical assistance.

References

Burdyga G, Varro A, Dimaline R, Thompson DG & Dockray GJ 2006 Ghrelin receptors in rat and human nodose ganglia: putative role in regulating CB-1 and MCH receptor abundance. *American Journal of Physiology. Gastrointestinal and Liver Physiology* **290** G1289–G1297.

Cannon B & Nedergaard J 2004 Brown adipose tissue: function and physiological significance. *Physiological Reviews* **84** 277–359.

Cano G, Passerin AM, Schiltz JC, Card JP, Morrison SF & Sved AF 2003 Anatomical substrates for the central control of sympathetic outflow to interscapular adipose tissue during cold exposure. *Journal of Comparative Neurology* **460** 303–326.

Champigny O & Ricquier D 1990 Effects of fasting and refeeding on the level of uncoupling protein mRNA in rat brown adipose tissue: evidence for diet-induced and cold-induced responses. *Journal of Nutrition* **120** 1730–1736.

Currie PJ, Mirza A, Fuld R, Park D & Vasselli JR 2005 Ghrelin is an orexigenic and metabolic signaling peptide in the arcuate and paraventricular nuclei. *American Journal of Physiology. Regulatory, Integrative and Comparative Physiology* **289** 353–358.

Date Y, Murakami N, Kojima M, Kuroiwa T, Matsukura S, Kangawa K & Nakazato M 2000 Central effects of a novel acylated peptide, ghrelin, on growth hormone release in rats. *Biochemical and Biophysical Research Communications* **275** 477–480.

Date Y, Murakami N, Toshinai K, Matsukura S, Niijima A, Matsuo H, Kangawa K & Nakazato M 2002 The role of the gastric afferent vagal nerve in ghrelin-induced feeding and growth hormone secretion in rats. *Gastroenterology* **123** 1120–1128.

Date Y, Shimbara T, Koda S, Toshinai K, Ida T, Murakami N, Miyazato M, Kokame K, Ishizuka Y, Ishida Y *et al.* 2006 Peripheral ghrelin transmits orexigenic signals through the noradrenergic pathway from the hindbrain to the hypothalamus. *Cell Metabolism* **4** 1–9.

Gabaldón AM, Gavel DA, Hamilton JS, McDonald RB & Horwitz BA 2003 Norepinephrine release in brown adipose tissue remains robust in cold-exposed senescent Fischer 344 rats. *American Journal of Physiology. Regulatory, Integrative and Comparative Physiology* **285** R91–R98.

Howard AD, Feighner SD, Cully DF, Arena JP, Liberator PA, Rosenblum CI, Hamelin M, Hreniuk DL, Palyha OC, Anderson J *et al.* 1996 A receptor in pituitary and hypothalamus that functions in growth hormone release. *Science* **273** 974–977.

Kobelt P, Tebbe JJ, Tjandra I, Stengel A, Bae H, Anderson V, Voort IR, Veh RW, Werner CR, Klapp BF *et al.* 2005 CCK inhibits orexigenic effect of peripheral ghrelin. *American Journal of Physiology. Regulatory, Integrative and Comparative Physiology* **288** R751–R758.

Kojima M, Hosoda H, Date Y, Nakazato M, Matsuo H & Kangawa K 1999 Ghrelin is a growth-hormone-releasing acylated peptide from stomach. *Nature* **402** 656–660.

Lawrence CB, Snape AC, Baudoin FM & Luckman SM 2002 Acute central ghrelin and GH secretagogues induce feeding and activate brain appetite centers. *Endocrinology* **143** 155–162.

Lee HM, Wang G, Englander EW, Kojima M & Greeley GH Jr 2002 Ghrelin, a new gastrointestinal endocrine peptide that stimulates insulin secretion: enteric distribution, ontogeny, influence of endocrine, and dietary manipulations. *Endocrinology* **143** 185–190.

Lowell BB & Spiegelman BM 2000 Towards a molecular understanding of adaptive thermogenesis. *Nature* **404** 652–660.

Mano-Otagiri A, Nemoto T, Sekino A, Yamauchi N, Shuto Y, Sugihara H, Oikawa S & Shibasaki T 2006 Growth hormone-releasing hormone (GHRH) neurons in the arcuate nucleus (Arc) of the hypothalamus are decreased in transgenic rats whose expression of ghrelin receptor is attenuated: evidence that ghrelin receptor is involved in the up-regulation of GHRH expression in the Arc. *Endocrinology* **147** 4093–4103.

McKee KK, Palyha OC, Feighner SD, Hreniuk DL, Tan CP, Phillips MS, Smith RG, Van der Ploeg LH & Howard AD 1997 Molecular analysis of rat pituitary and hypothalamic growth hormone secretagogue receptors. *Molecular Endocrinology* **11** 415–423.

Murakami N, Hayashida T, Kuroiwa T, Nakahara K, Ida T, Mondal MS, Nakazato M, Kojima M & Kangawa K 2002 Role for central ghrelin in food intake and secretion profile of stomach ghrelin in rats. *Journal of Endocrinology* **174** 283–288.

Nakazato M, Murakami N, Date Y, Kojima M, Matsuo H, Kangawa K & Matsukura S 2001 A role for ghrelin in the central regulation of feeding. *Nature* **409** 194–198.

Okada K, Ishii S, Minami S, Sugihara H, Shibasaki T & Wakabayashi I 1996 Intracerebroventricular administration of the growth hormone-releasing peptide KP-102 increases food intake in free-feeding rats. *Endocrinology* **137** 5155–5158.

Oldfield BJ, Giles ME, Watson A, Anderson C, Colvill LM & Mckinley MJ 2002 The neurochemical characterisation of hypothalamic pathways projecting polysynaptically to brown adipose tissue in the rat. *Neuroscience* **110** 515–526.

Paxinos G & Watson C 1996 *The Rat Brain in Stereotaxic Coordinates*. edn 3, San Diego: Academic press.

Rüter J, Kobelt P, Tebbe JJ, Avsar Y, Veh R, Wang L, Klapp BF, Wiedenmann B, Taché Y & Mönnikes H 2003 Intraperitoneal injection of ghrelin induces Fos expression in the paraventricular nucleus of the hypothalamus in rats. *Brain Research* **991** 26–33.

Sakata I, Yamazaki M, Inoue K, Hayashi Y, Kangawa K & Sakai T 2003 Growth hormone secretagogue receptor expression in the cells of the stomach-projected afferent nerve in the rat nodose ganglion. *Neuroscience Letters* **342** 183–186.

Shuto Y, Shibasaki T, Otagiri A, Kuriyama H, Ohata H, Tamura H, Kamegai J, Sugihara H, Oikawa S & Wakabayashi I 2002 Hypothalamic growth hormone secretagogue receptor regulates growth hormone secretion, feeding, and adiposity. *Journal of Clinical Investigation* **109** 1429–1436.

Smith GP, Jerome C, Cushin BJ, Eterno R & Simansky KJ 1981 Abdominal vagotomy blocks the satiety effect of cholecystokinin in the rat. *Science* **213** 1036–1037.

Smith RG, Van der Ploeg LHT, Howard AD, Feighner SD, Cheng K, Hickey GJ, Wyvratt MJ Jr, Fisher MH, Nargund RP & Patchett AA 1997 Peptidomimetic regulation of growth hormone secretion. *Endocrine Reviews* **18** 621–645.

Surwit RS, Dixon TM, Petro AE, Daniel KW & Collins S 2000 Diazoxide restores β3-adrenergic receptor function in diet-induced obesity and diabetes. *Endocrinology* **141** 3630–3637.

Tamura H, Kamegai J, Shimizu T, Ishii S, Sugihara H & Oikawa S 2002 Ghrelin stimulates GH but not food intake in arcuate nucleus ablated rats. *Endocrinology* **143** 3268–3275.

Tannenbaum GS, Epelbaum J & Bowers CY 2003 Interrelationship between the novel peptide ghrelin and somatostatin/growth hormone-releasing hormone in regulation of pulsatile growth hormone secretion. *Endocrinology* **144** 967–974.

Theander-Carrillo C, Wiedmer P, Cettour-Rose P, Nogueiras R, Perez-Tilve D, Pfluger P, Castaneda TR, Muzzin P, Schürmann A, Szanto I *et al.* 2006 Ghrelin action in the brain controls adipocyte metabolism. *Journal of Clinical Investigation* **116** 1983–1993.

Thrivikraman KV, Huot RL & Plotsky PM 2002 Jugular vein catheterization for repeated blood sampling in the unrestrained conscious rat. *Brain Research Protocols* **10** 84–94.

Tschöp M, Smiley DL & Heiman ML 2000 Ghrelin induces adiposity in rodents. *Nature* **407** 908–913.

Tsubone T, Masaki T, Katsuragi I, Tanaka K, Kakuma T & Yoshimatsu H 2005 Ghrelin regulates adiposity in white adipose tissue and UCP1 mRNA expression in brown adipose tissue in mice. *Regulatory Peptides* **130** 97–103.

Yasuda T, Masaki T, Kakuma T & Yoshimatsu H 2003 Centrally administered ghrelin suppresses sympathetic nerve activity in brown adipose tissue of rats. *Neuroscience Letters* **349** 75–78.

Young JB, Saville E, Rothwell NJ, Stock MJ & Landsberg L 1982 Effect of diet and cold exposure on norepinephrine turnover in brown adipose tissue of the rat. *Journal of Clinical Investigation* **69** 1061–1071.

Zigman JM, Jones JE, Lee CE, Saper CB & Elmquist JK 2006 Expression of ghrelin receptor mRNA in the rat and the mouse brain. *Journal of Comparative Neurology* **494** 528–548.

Received in final form 12 March 2009
Accepted 6 April 2009
Made available online as an Accepted Preprint
7 April 2009

Regulatory Peptides 160 (2010) 81–90

Contents lists available at ScienceDirect

Regulatory Peptides

journal homepage: www.elsevier.com/locate/regpep

Genetic suppression of ghrelin receptors activates brown adipocyte function and decreases fat storage in rats

Asuka Mano-Otagiri [a,*], Azusa Iwasaki-Sekino [a], Takahiro Nemoto [a], Hisayuki Ohata [a], Yujin Shuto [b], Hajime Nakabayashi [c], Hitoshi Sugihara [b], Shinichi Oikawa [b], Tamotsu Shibasaki [a]

[a] Departments of Physiology, Nippon Medical School, 1-1-5 Sendagi, Bunkyo-ku, Tokyo 113-8602, Japan
[b] Medicine, Nippon Medical School, 1-1-5 Sendagi, Bunkyo-ku, Tokyo 113-8602, Japan
[c] Division of Life Science, Graduate School of Natural Science and Technology and Health Science Service Center, Kanazawa University, Kakuma, Kanazawa 920-1192, Japan

ARTICLE INFO

Article history:
Received 23 July 2009
Received in revised form 6 November 2009
Accepted 12 November 2009
Available online 18 November 2009

Keywords:
Energy metabolism
Brown adipose tissue
White adipose tissue
Thermogenesis
Vagal afferent

ABSTRACT

To clarify the role of ghrelin and its receptor (GHS-R) in the regulatory mechanism of energy metabolism, we analyzed transgenic (Tg) rats expressing an antisense GHS-R mRNA under the control of the tyrosine hydroxylase (TH) promoter. Tg rats showed lower visceral fat weight and higher O_2 consumption, CO_2 production, rectal temperature, dark-period locomotor activity, brown adipose tissue (BAT) weight and uncoupling protein 1 expression compared with wild-type (WT) rats on a standard diet. A high-fat diet for 14 days significantly increased body weight, visceral fat weight, and the sizes of white and brown adipocytes in WT rats but not in Tg rats compared with the corresponding standard-diet groups. Antisense GHS-R mRNA was expressed and GHS-R expression was reduced in TH-expressing cells of the vagal nodose ganglion in Tg rats. Ghrelin administered intravenously suppressed noradrenaline release in the BAT of WT rats, but not in Tg rats. These results suggest that ghrelin/GHS-R plays an important role in energy storage by modifying BAT function and locomotor activity. As our previous study showed that peripheral ghrelin-induced noradrenaline release suppression in BAT is blocked by vagotomy, the present findings also suggest that vagal afferents transmit the peripheral ghrelin signal to the sympathetic nervous system innervating BAT.

1. Introduction

Ghrelin was isolated from rat stomach extracts [1] as an endogenous ligand for the growth hormone secretagogue (GHS) receptor (GHS-R) [2]. Ghrelin/GHSs stimulate not only growth hormone (GH) secretion but also food intake through the GHS-R when administered intracerebroventricularly (icv) and peripherally [3–6]. Ghrelin administered icv or peripherally increases the respiratory quotient (RQ), indicating an inhibitory action of ghrelin on fat oxidation [6]. Brown adipocytes increase energy expenditure by thermogenesis, and their activity is regulated by the sympathetic nerves [7]. ICV administration of ghrelin suppresses sympathetic efferent activity to brown adipose tissue (BAT) [8]. These findings suggest that ghrelin induces positive energy balance not only by increasing food intake but also by decreasing energy expenditure. Noradrenaline released from the sympathetic nerve endings in BAT binds to β_3-adrenergic receptors on brown adipocytes and initiates intracellular breakdown of triglyceride to free fatty acid by activating hormone-sensitive lipase through an intracellular signal, cAMP. Free fatty acids are substrates for thermogenesis and activators of uncoupling protein 1 (UCP1). UCP1 is highly expressed in brown adipocytes and is involved in thermogenesis in BAT [9].

However, the details of endogenous ghrelin/GHS-R function in the regulatory mechanism of energy metabolism remain unclear. Studies using ghrelin-null mice did not show any significant changes in body weight, food intake, body fat, O_2 consumption (VO_2), or RQ on a standard diet (SD); thus, the physiological significance of ghrelin remains unknown [10,11]. In another study, 16-week-old GHS-R-null mice on a SD showed significantly lower body weight and serum IGF-I levels than control littermates, although there were no significant changes in food intake, core body temperature, metabolic rate, or body fat mass [12]. To further explore the role of endogenous ghrelin and GHS-R in the regulatory mechanism of energy metabolism, the effects of a high-fat diet (HFD) on energy metabolism in ghrelin-null mice or GHS-R-null mice were examined by several research groups [11,13,14]. The common phenotype of these KO mice on a HFD is resistance to obesity. These studies indicated that the physiological significance of ghrelin/GHS-R becomes evident when Tg animals lacking ghrelin or GHS-R are fed a HFD, although the changes in indices concerning energy metabolism were not the same among the different research groups.

We previously created transgenic (Tg) rats expressing an antisense GHS-R mRNA under the control of the promoter for tyrosine

* Corresponding author. Department of Physiology, Nippon Medical School, 1-1-5 Sendagi, Bunkyo-ku, Tokyo 113-8602, Japan. Tel.: +81 3 3822 2131; fax: +81 3 3822 0766.
E-mail address: asuka@nms.ac.jp (A. Mano-Otagiri).

0167-0115/$ – see front matter © 2009 Elsevier B.V. All rights reserved.
doi:10.1016/j.regpep.2009.11.010

hydroxylase (TH) [5]. TH-positive neurons are located in the arcuate nucleus (Arc) of the hypothalamus, where growth hormone-releasing hormone (GHRH) neurons, target neurons for ghrelin/GHSs to stimulate GH secretion, are also located. Our Tg rats showed less GHS-R protein in the Arc [5] and fewer GHRH neurons expressing GHS-R compared with WT rats [15]. In addition, female Tg rats showed lower GH secretion and lower serum IGF-I levels [5]. These results suggest that GHS-R in the Arc plays an important role in the regulatory mechanism of GH secretion. The Tg rats also showed lower body weight at birth and less white adipose tissue (WAT) mass than WT rats on a SD; this phenotype is completely different from those of the other genetically modified animals lacking ghrelin or GHS-R described above. In the present study, using our Tg rats, we tried to further clarify the role of ghrelin/GHS-R in the regulatory mechanism of energy metabolism, especially in brown adipocytes, which are important for energy expenditure. For this purpose, the weight of WAT and BAT, UCP1 expression in BAT, which is a marker of BAT activity, VO_2, CO_2 production (VCO_2), RQ, rectal temperature, and locomotor activity were compared between Tg and WT rats on a SD or HFD. Since several studies have shown that GHS-R is expressed in the vagal nodose ganglion [16–18], and we have previously clarified that intravenous (iv) administration of ghrelin suppresses noradrenaline release in BAT of normal rats in a manner dependent on vagal signaling [19], we also analyzed the expression of antisense GHS-R and the expression levels of GHS-R in the vagal nodose ganglion and tested the effect of iv ghrelin on noradrenaline release in BAT in the Tg rats.

2. Materials and methods

2.1. Animals

Homozygous Tg rats were generated from Sprague–Dawley rats (SLC, Shizuoka, Japan) as described previously [5]. Male Tg rats and age-matched male Sprague–Dawley rats (7–8 weeks) were used in this study. The rats were housed individually in each cage (20×25×18 cm) and maintained at 24 °C on a 12:12-h light–dark cycle (lights on at 0800 h, off at 2000 h). They were allowed ad libitum access to laboratory chow and distilled water. All experimental procedures were conducted in accordance with the guidelines for use and care of Laboratory Animals Ethics Committee of Nippon Medical School.

2.2. HFD loading

Eight-week-old rats were fed either with a SD (12% fat, 20% protein, and 65% carbohydrate; Nosan Corp., Kanagawa, Japan) or a HFD (45% fat, 16% protein, and 34% carbohydrate; Nosan Corp.) for 14 days. Daily food intake and body weight were measured at 0900 h every day throughout the 14 days.

2.3. VO_2 and VCO_2

On day 15, VO_2 and VCO_2 of the WT and Tg rats that had been fed with a SD or HFD for 14 days were measured sequentially with an open-circuit-type O_2/CO_2 metabolism measuring system (Model MK-5000; Muromachikikai, Tokyo, Japan). Each rat was kept unrestrained in a sealed chamber (1500-ml volume) without food or water, with constant air flow of 1500 ml/min, for 2 h between 1200 and 1400 during the light cycle, at 24 °C. Air samples from two acrylic chambers, in each of which a WT rat or Tg rat was alternately placed, were simultaneously and continuously taken every 3 min, and the concentrations of O_2 and CO_2 recorded. VO_2 and VCO_2 were determined as milliliters per minute per kilogram body weight when the minimum plateau shape was obtained. The mean RQ, the ratio of VCO_2/VO_2, was calculated from continuous 10-point data. The analyzer was calibrated before each use with primary gas standards of high purity.

2.4. Rectal temperature

On day 15, rectal temperature was measured using an electric thermometer (Natume Seisakusho, Tokyo, Japan) with an inserting probe placed in the rectum.

2.5. Locomotor activity

An automatic behavioral measurement system (PAW-2000, Melquest, Toyama, Japan) was used to measure the locomotor activity of the rats for 24 h during the 14-day exposure to a SD or HFD. The apparatus consisted of individual cages (30×30×38 cm) equipped with a horizontal 5×5 array of infrared beams 2 cm above the floor.

2.6. Blood and adipose tissue sampling

On day 15, the rats were killed by decapitation, and then trunk blood was collected. Visceral fat (mesenteric, retroperitoneal, and epididymal) and BAT were immediately removed. The weight of each tissue was measured, and then BAT was stored at −80 °C for later analysis of UCP1 expression. After centrifugation, plasma samples were stored at −20 °C until use.

2.7. Determination of plasma leptin and IGF-I concentrations

Plasma concentrations of leptin were measured using a rat leptin ELISA kit (Wako Pure Chemical Industries, Ltd., Osaka, Japan). Plasma IGF-I levels were determined with a mouse IGF-I immunoassay kit (R&D Systems, Minneapolis, MN).

2.8. Histology

On day 15, the rats for histological studies were deeply anesthetized with an intraperitoneal (ip) injection of sodium pentobarbital (50 mg/kg of body weight) and perfused via an intracardiac cannula with PBS followed by 4% paraformaldehyde. After being post-fixed in paraformaldehyde overnight, WAT samples from the mesenteric region and BAT samples were embedded in paraffin and cut into 2-μm-thick sections. The sections were stained with hematoxylin–eosin. The size and number per 1 mm^2 of white adipocytes and brown adipocytes in these samples were counted in three randomly selected fields of each stained specimen. The image was captured (microscope; BX50, objective lens; ×40 OLYMPUS, Tokyo, Japan, camera; Power HAD, SONY, Tokyo, Japan) and analyzed using an image analysis system (MCID Elite Version 6.0, Imaging Research Inc., Ontario, Canada).

2.9. Northern blotting analysis of UCP1 mRNA in BAT

UCP1 cDNA was amplified from BAT RNA using 5′-CCGGATC-CAGGCTTCCAGTACTATTAG-3′ (sense) and 5′-CCGAATTCGCCACCCGT-CATCAAGCCA-3′ (antisense) primers, which range from position 310 to 547 (NCBI: BC088156). The amplified cDNA was subcloned into pGEM 3Z vector (Promega, Madison, WI). Plasmid vector was digested by Eco RI and Bam HI, and the 233-bp UCP1 cDNA fragment was then labeled using the digoxigenin (DIG) DNA labeling and detection kit (Roche Diagnostics GmbH, Mannheim, Germany). A 20-μg amount of total RNA was separated with 0.8% agarose gel and transferred to a positively charged nylon membrane. The membranes were fixed by UV crosslinking and prehybridized in high SDS buffered solution (7% SDS, 50% formamide, 5× saline sodium citrate [SSC], 50 mM sodium phosphate, pH 7.0, 0.1% N-Lauroylsarcosine, and 50 μg/ml yeast tRNA) at 55 °C for 2 h. DIG-labeled DNA probe was added and hybridized at

55 °C for 48–72 h. The membranes were then washed and primed with anti-DIG antibody conjugated with alkaline phosphatase. The signals were detected on Fuji Las 1000 (Fujifilm, Tokyo, Japan) using CDP star detection reagent (Amersham Bioscience, Buckinghamshire, UK). Quantification of the bands was performed using NIH image software (developed by Dr. Wayne Rasband; available via http://rsb.info.nih.gov), and the intensity of the bands was normalized using the density of the 18S rRNA bands.

2.10. RT-PCR of antisense GHS-R in the vagal nodose ganglion

Eight-week-old male Tg and WT rats were anesthetized with an ip injection of sodium pentobarbital (50 mg/kg of body weight), and vagal nodose ganglion were dissected and processed as described below. Total RNA was isolated from the bilateral vagal nodose ganglions of WT and Tg rats using Isogen (Nippon Gene, Tokyo, Japan). To avoid false positive results caused by DNA contamination, samples were treated with RNase-free DNase (Takara, Shiga, Japan) at 37 °C for 60 min. First strand cDNA was synthesized using 1 μg denatured total RNA at 42 °C for 60 min, at 99 °C for 5 min, and at 5 °C for 5 min. PCR was performed by 40 cycles of denaturation at 94 °C for 30 s, annealing at 50 °C for 30 s, and extension at 72 °C for 60 s, using specific primers for rat GHS-R antisense or GHS-R. Antisense GHS-R mRNA was detected using RT-PCR, as described previously [5]. After amplification, the PCR products were subjected to 2% agarose gel electrophoresis, stained with 0.5 μg/ml ethidium bromide, and visualized under ultraviolet illumination. The intensity of the GHS-R PCR product band was quantified using NIH Image software and normalized to the intensity of the β-actin band that was simultaneously amplified. All PCR-amplified DNAs were confirmed by sequencing.

2.11. Western blotting analyses of UCP1 in BAT and GHS-R in the vagal nodose ganglion

Tissues were homogenized with a sonicator in TNE buffer (10 mM Tris–HCl, pH 7.8, 1% NP-40, 150 mM NaCl, and 1 mM EDTA) containing the Complete™ proteinase inhibitor cocktail (Roche Diagnostics GmbH). After centrifugation, protein concentrations in the supernatant were measured. Protein extracts (20 μg) were mixed with 3× SDS-sample buffer (30% glycerol, 6% SDS, 200 mM Tris–HCl, pH 6.8, 0.03% bromophenol blue, and 3% β-mercaptoethanol) and boiled for 5 min. Proteins in the extracts were then separated by SDS-PAGE and transferred onto PVDF membranes (Bio-Rad, Hercules, CA). The membranes were blocked with 5% nonfat dried milk at room temperature for 30 min and primed with anti-UCP1 antibody (1:1000, Calbiochem, San Diego, CA) for UCP1 in BAT, or with GHS-R antibody [20] for GHS-R in the vagal nodose ganglion, at room temperature for 1 h. The membranes were washed three times with TBST (10 mM Tris–HCl, pH 7.4, 150 mM NaCl, 0.05% Tween 20) and then incubated with HRP-conjugated anti-rabbit IgG antibody (1:10,000, Jackson Immuno Research Laboratories, Inc., West Grove, PA) at room temperature for 1 h. The membranes were washed five times with TBST. Immunoreactivity was detected on Fuji Las 1000 (Fujifilm) using Super Signal Ultra Chemiluminescent Substrate (Pierce, Rockford, IL). The intensities of the bands were measured using NIH Image software Ver 1.63f.

2.12. In situ hybridization for antisense GHS-R and TH in the vagal nodose ganglion

To construct an RNA probe for TH and a GHS-R antisense probe, a 475-bp fragment of the rat TH gene that was amplified by RT-PCR and a synthetic 108-nucleotide DNA fragment of the GHS-R gene, respectively, were subcloned into pGEM-T Easy Vector (Promega). The resultant plasmid vectors were digested by restriction enzyme Nco I or Sal I, respectively, at 37 °C for 1 h. They were then labeled using the Biotin RNA Labeling Mix and DIG RNA Labeling Kit (Roche Diagnostics GmbH), as described previously [5].

For histological analysis of expression of GHS-R antisense or TH in the vagal nodose ganglion, WT and Tg rats were perfused as described above. After being post-fixed in paraformaldehyde overnight, the tissues were embedded in paraffin and cut into 4-μm-thick sections, dewaxed, and dehydrated. Each slide was covered with a coverslip with 50 μl of hybridization solution (50% formamide, 5× SSC, 50 μg/ml yeast total RNA, 1% SDS, and 50 μg/ml heparin) containing 1 μg/ml of DIG-labeled riboprobe. The slides were incubated in a humidified oven overnight at 37 °C, washed twice in 5× SSC/1% SDS/50% formamide at 37 °C for 30 min, washed three times in 0.5 M NaCl/10 mM Tris–HCl (pH 7.5) at room temperature for 10 min, and then washed twice in 2× SSC/50% formamide at 37 °C for 30 min. The DIG-labeled probe was detected by incubation with antibody conjugated with alkaline phosphatase (Roche Diagnostics GmbH) at room temperature for 60 min. The slides were washed and developed with NBT/BCIP (Roche Diagnostics GmbH) at room temperature for 36–48 h. Slides were then mounted with Aquatex (Merck, Darmstadt, Germany) and the image was captured (microscope; BX50, objective lens; ×40 OLYMPUS, Tokyo, Japan, camera; Power HAD, SONY, Tokyo, Japan).

For double-labeled in situ hybridization, hybridization of GHS-R antisense was performed as described above. Qdot565 sheep anti-DIG conjugate [Fab fragment] (1:100, Quantum Dot Corporation, Hayward, CA) was applied, and slides were incubated at 37 °C for 3 h. The sections were washed in PBS and subsequently hybridized using biotin-labeled riboprobe for TH overnight at 37 °C, and then the hybridization signal was detected by incubation with Qdot655 streptavidin conjugate (1:100, Quantum Dot) at 37 °C for 3 h. The slides were coverslipped with VectaShield Hard Set mounting medium (Vector Laboratories, Burlingame, CA).

2.13. Double-labeled immunohistochemistry for GHS-R and TH in the vagal nodose ganglion

Double-labeled immunofluorescent staining for GHS-R and TH coupled with confocal microscopic analysis was performed with paraffin-embedded sections of the vagal nodose ganglion. The sections were incubated with antiserum against GHS-R (1:10) overnight at 4 °C, as described previously [20]. The sections were then rinsed in PBS and incubated with fluorescein-conjugated goat anti-rabbit IgG (1:200, Vector Laboratories) at room temperature for 3 h. The sections were washed in PBS and subsequently incubated overnight at 4 °C with the second antibody, antiserum against TH (1:100, AB151; Chemicon International, Temecula, CA). After washing in PBS, the sections were incubated in Texas red-conjugated goat anti-rabbit IgG (1:200, Vector Laboratories) at room temperature for 3 h. The slides were coverslipped with Vectashield hard set mounting medium (Vector Laboratories).

2.14. Detection of immunofluorescence in the vagal nodose ganglion

The sections were examined using a Zeiss LSM 510 confocal microscope system (Carl Zeiss Co. Ltd., Thornwood, NY) to detect immunofluorescence in the tissue sections with a multiband filter set for independent or simultaneous visualization of Qdot565 or fluorescein (excitation range: 447–501 nm, emission range: 510–540 nm) and Qdot655 or Texas red (excitation range: 560–596 nm, emission range: 610–655 nm). All images were processed with Adobe Photoshop software (Adobe Systems, San Jose, CA).

2.15. Microdialysis for assay of noradrenaline in the BAT

Four days before the experiment, an iv catheter was inserted into the right external jugular vein of the rats under ip sodium

pentobarbital anesthesia (50 mg/kg of body weight) [21]. On the day of the experiment, a linear microdialysis probe (OP-100-05; Eicom Corp., Kyoto, Japan) with 5-mm dialyzable membrane was implanted into the interscapular BAT under light anesthesia with ether [19]. The skin in the interscapular area was shaved and cleaned with 70% ethanol, and a small incision was made along the midline, exposing a deposit of white fat and underlying interscapular brown fat. A microdialysis probe was inserted into either lobe of the brown fat lobes. The end of the probe was exteriorized through a midscapular skin incision, and the skin incision was then sutured closed. After the rat had recovered from anesthesia, the probe was connected with tubing for microdialysis, and microdialysis was performed under free-moving conditions between 1100 h and 1800 h. The probe was continuously perfused with Ringer's solution (147 mM NaCl, 4 mM KCl, and 2.3 mM $CaCl_2$, pH 7.0) at a flow rate of 2 μl/min and the dialysate was collected every 20 min. Noradrenaline concentrations in dialysates (40 μl/20 min) were determined by a combination of HPLC and electrochemical detection using an Eicompak CA-5ODS column (2.1 mm i.d. × 150 mm; Eicom Corp.) and a WE-3G graphite electrode (Eicom Corp.) set at +450 mV against an Ag/AgCl reference electrode. The current sensitivity was 0.1 nA. The mobile phase in the HPLC column was 0.1 M sodium phosphate buffer (pH 6.0) containing 1.85 mM sodium octanesulfonic acid, 0.17 mM EDTA, and 5.0% (v/v) methanol. After a 3-h-stabilization period, baseline noradrenaline levels were defined as the average release in three consecutive fractions immediately preceding the injection and were considered as 100%. Rats then received an iv injection of 30 nmol of rat ghrelin (Peptide Institute, Inc., Osaka, Japan). The ghrelin dose was determined by its action to suppress noradrenaline release in BAT in WT rats [19].

2.16. Data analysis

All results are expressed as mean ± SEM. The data of daily body weight gain was subjected to three-way repeated-measures ANOVA with genotype, type of food, and day as factors. The data of total caloric intake, fat weight, size and cell number of adipose tissue, VO_2, VCO_2, RQ, rectal temperature, UCP1 expression, plasma leptin and IGF-I concentration, were subjected to two-way ANOVA with genotype and type of food as factors. The data from microdialysis was subjected to three-way repeated-measures ANOVA with genotype, ghrelin injection, and time as factors. Subsequently, Fisher's PLSD test for multiple comparisons was used. Tukey–Kramer post-hoc analysis was used for comparison of locomotor activity data. An unpaired t-test was used for comparison of GHS-R expression in the vagal nodose ganglion. P values less than 0.05 were considered statistically significant.

3. Results

3.1. Body weight and total caloric intake

As the body weights of each group on day 1 were statistically different (Tg-SD, 203.8 ± 14.3 g; Tg-HFD, 208.2 ± 12.8 g; WT-SD, 247.9 ± 13.3 g; WT-HFD, 254.1 ± 13.6 g; $F_{1,\ 48} = 11.12$, $P<0.01$), the cumulative body weight gains were used for the statistical analysis. The daily body weight gains of WT and Tg rats on the SD or HFD are shown in Fig. 1A. There were significant interactions among genotype, type of food and day ($F_{13,\ 624} = 3.31$, $P<0.001$). The subsequent analysis revealed that the HFD loading significantly increased body weight gain in WT rats from day 7 to day 14 ($P<0.05$), but not in Tg rats. The total caloric intake of each group during 14 days is shown in Fig. 1B. There were main effects of genotype ($F_{1,\ 26} = 8.72$, $P<0.01$) and type of food ($F_{1,\ 26} = 7.09$, $P<0.05$) on the total caloric intake. Further analysis revealed that the total caloric intake of Tg rats on the SD was lower than that of WT rats on the SD ($P<0.05$), and that the HFD increased caloric intake both in WT and Tg rats ($P<0.05$).

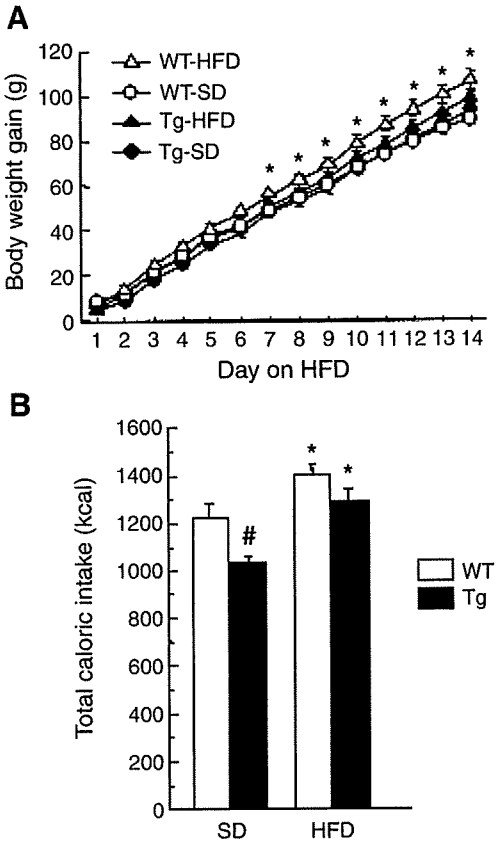

Fig. 1. Cumulative daily body weight gain and total caloric intake during HFD loading. (A) From day 7 to day 14, cumulative body weight gains of WT rats on the HFD were significantly higher compared to WT rats on the SD. HFD loading induced no significant change in body weight gains of Tg rats. Data are shown as mean ± SEM. The number of rats in each group was 13. (B) On the SD, total caloric intake was lower in Tg rats than in WT rats. Total caloric intake during the 14 days was increased by HFD loading in both groups. Data are shown as mean ± SEM. The number of rats in each group was 7–8. *$P<0.05$, compared with each SD group; #$P<0.05$, compared with WT rats on the SD.

3.2. Changes in tissue weight and size and density of white and brown adipocytes

After the 2-week HFD-loading experiment, the weight of visceral WAT and BAT were examined. There was a significant interaction between genotype and type of food in visceral fat weight ($F_{1,\ 48} = 4.75$, $P<0.05$). As shown in Fig. 2A, subsequent analysis revealed that HFD loading significantly increased visceral fat weight in WT rats ($P<0.01$) but not in Tg rats. In contrast to WAT, BAT weight significantly increased after the HFD loading in Tg rats ($P<0.05$) but not in WT rats (Fig. 2B).

The effect of HFD loading on adipose tissues was supported by the histological analysis on the size and density of adipocytes. There were significant main effects of genotype ($F_{1,\ 26} = 37.39$, $P<0.0001$) and type of food ($F_{1,\ 26} = 8.64$, $P<0.01$) on the size of white adipocytes. As shown in Fig. 2C, HFD increased the size of white adipocytes in WT rats. In the number of white adipocytes per mm^2, there was a significant interaction between genotype and type of food ($F_{1,\ 26} = 7.76$, $P = 0.01$). Further analysis revealed that HFD significantly decreased the number of white adipocytes per mm^2 in WT rats ($P<0.05$) but not in Tg rats (Fig. 2D). In contrast, the interaction between genotype and type of food on the size of brown adipocytes was significant ($F_{1,\ 20} = 8.43$, $P<0.01$). Further analysis confirmed that HFD increased the size of brown adipocytes in WT rats ($P<0.05$) but not in Tg rats (Fig. 2E). There was a main effect of

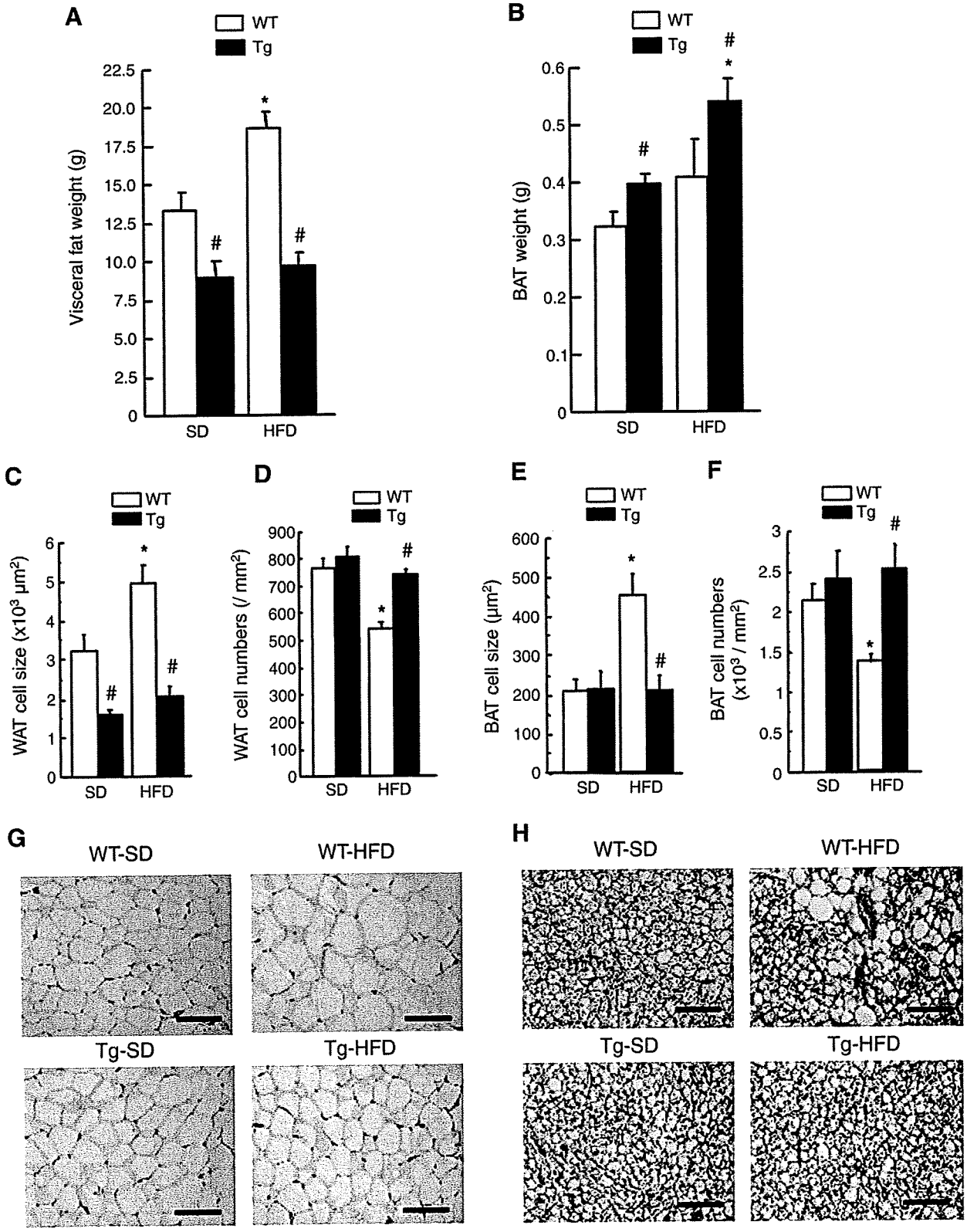

Fig. 2. Effects of HFD loading on adipose tissue. HFD loading significantly increased visceral fat weight in WT rats but not in Tg rats (A), and BAT weight in Tg rats but not in WT rats (B). In WT rats, HFD loading significantly increased the size of white adipocytes (C) and brown adipose (E), and decreased the density of white adipocytes (D) and brown adipocytes (F), although no significant change was observed in Tg rats either in the size of white adipocytes (C) or brown adipocytes (E), or in the density of white adipocytes (D) or brown adipocytes (F). Data are shown as mean ± SEM. The number of rats in each group was 7–8. *$P<0.05$, compared with SD within the same genotype. #$P<0.05$, compared with WT rats within the same diet. Microphotographs of mesenteric WAT (G) and BAT (H) in WT and Tg rats. The sections of white adipocytes and brown adipocytes were stained with hematoxylin–eosin. Scale bars, 100 μm.

genotype on the number of brown adipocytes per mm^2 ($F_{1,20}=7.44$, $P<0.05$). Further analysis revealed that HFD decreased the number of brown adipocytes per mm^2 in WT rats ($P<0.001$), but not in Tg rats (Fig. 2F).

Representative images of white adipocytes and brown adipocytes from WT and Tg rats after the HFD-loading experiment are shown in Fig. 2G and H, respectively.

3.3. VO_2, VCO_2, RQ, rectal temperature, and locomotor activity

VO_2, VCO_2, RQ, rectal temperature, and locomotor activity were analyzed to determine the difference in energy expenditure between WT and Tg rats after HFD loading. There was a main effect of genotype on VO_2 ($F_{1,14}=16.54$, $P<0.01$). VO_2 was significantly higher in Tg rats than in WT rats ($P<0.05$) on either diet, although HFD loading did not change VO_2 in either genotype (Fig. 3A). On VCO_2, there were main effects of genotype ($F_{1,14}=9.86$, $P<0.01$) and type of food ($F_{1,14}=12.80$, $P<0.01$). Further analysis revealed that VCO_2 on the SD was higher in Tg rats than in WT rats ($P<0.05$), and that HFD loading significantly decreased VCO_2 both in WT rats and in Tg rats ($P<0.05$) (Fig. 3B). As shown in Fig. 3C, HFD loading significantly decreased RQ both in WT rats and in Tg rats ($F_{1,14}=17.22$, $P<0.01$) without a significant difference in RQ between the two genotypes (Fig. 3C).

There was a main effect of genotype on rectal temperature ($F_{1,14}=8.24$, $P<0.05$). Further analysis revealed that on the SD, rectal temperature was significantly higher in Tg rats than in WT rats ($P<0.05$) (Fig. 3D).

The locomotor activities of WT and Tg rats during the dark and light periods on the SD or HFD are shown in Fig. 3E. Locomotor activity was significantly higher in Tg rats than in WT rats during the dark period ($F_{1,37}=93.04$, $P<0.01$).

3.4. Expression of UCP1 in BAT

Northern blotting analysis for UCP1 mRNA and western blotting analysis for UCP1 protein in BAT are shown in Fig. 4A and B, respectively. Both UCP1 mRNA level and UCP1 protein level were significantly higher in Tg rats than in WT rats ($F_{1,24}=10.51$, $P<0.01$, $F_{1,24}=8.97$, $P<0.01$, respectively), There was no significant difference in UCP1 protein between Tg and WT rats on the SD. HFD loading did not change the UCP1 mRNA level or UCP1 protein level in WT or Tg rats.

3.5. Plasma leptin concentrations

The plasma concentrations of leptin after the 2-week HFD loading were analyzed (Fig. 4C). There were significant main effects of the type of food ($F_{1,27}=40.74$, $P<0.0001$) and genotype ($F_{1,27}=42.88$, $P<0.0001$). The subsequent analysis revealed that HFD loading significantly increased plasma concentrations of leptin in WT ($P<0.05$) and Tg rats ($P<0.05$), and that these were significantly lower in Tg rats than in WT rats on the SD ($P<0.05$) and HFD ($P<0.05$).

3.6. Plasma IGF-I concentrations

There was no significant main effect of either genotype or type of food on plasma IGF-I concentrations (Fig. 4D).

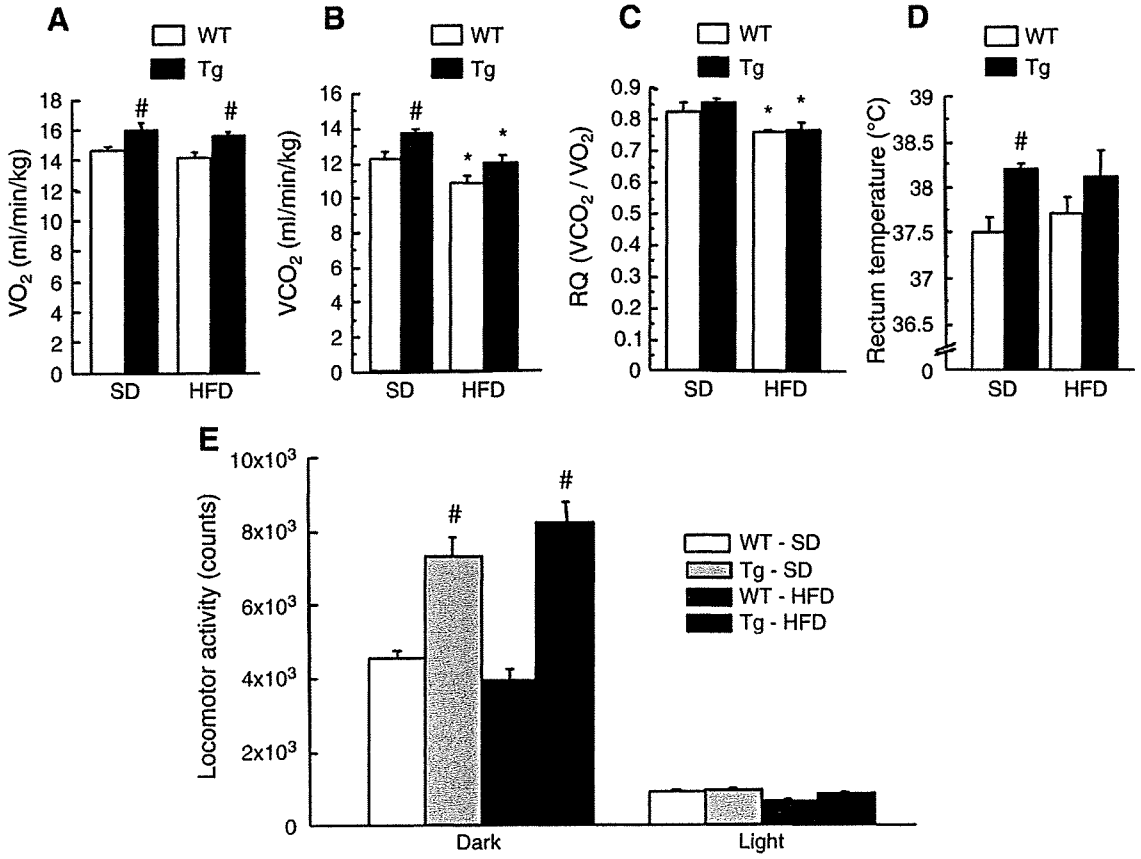

Fig. 3. Effects of HFD loading on the indices of energy metabolism. VO_2 (A), VCO_2 (B), rectum temperature (D) and locomotor activity during the dark phase (E) were significantly higher in Tg rats than in WT rats on the SD. HFD loading significantly decreased VCO_2 (B) and RQ (C). On the HFD, VO_2 and locomotor activity during the dark phase were significantly higher in Tg rats than in WT rats. Data are shown as mean ± SEM. The number of rats in each group was 4–6. *$P<0.05$, compared with SD within the same genotype. #$P<0.05$, compared with WT rats within the same diet.

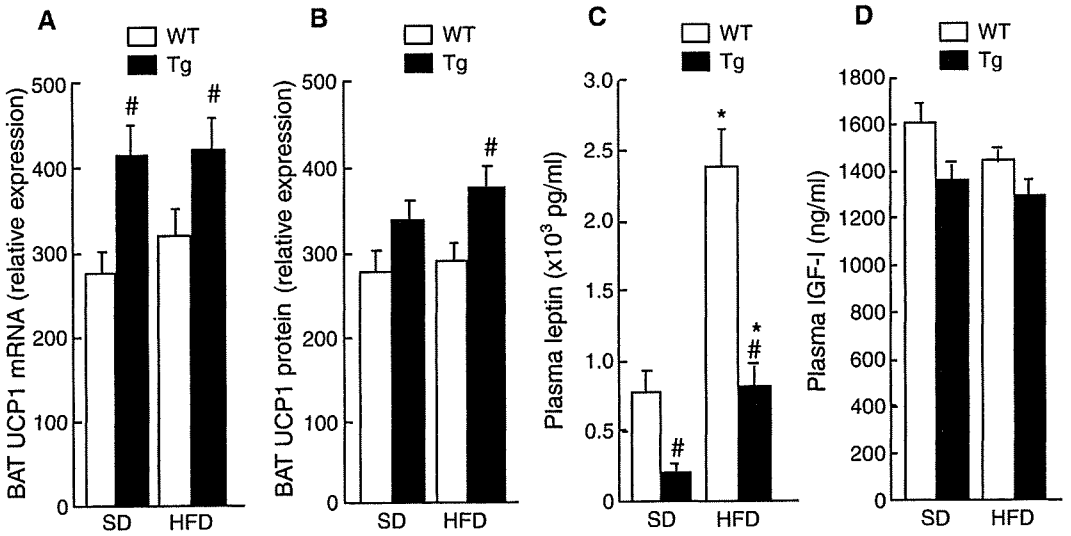

Fig. 4. Effects of HFD loading on the expression of BAT UCP1 and plasma leptin and IGF-I levels. The levels of BAT UCP1 mRNA (A) and UCP1 protein (B) were significantly higher in Tg rats than in WT rats. On the SD, plasma leptin levels were significantly lower in Tg rats than in WT rats, and 2 weeks of HFD loading significantly increased plasma leptin levels, more markedly in WT rats (C). No difference was observed in IGF-I levels (D). Data are shown as mean ± SEM. The number of rats in each group was 6–8. *$P<0.05$, compared with SD within same genotype. #$P<0.05$, compared with WT rats within the same diet.

3.7. TH, GHS-R antisense, and GHS-R expression in vagal nodose ganglion

Double immunohistochemical studies showed GHS-R expression on TH-expressing cell bodies in the vagal nodose ganglion of WT rats (Fig. 5A). The results of RT-PCR (Fig. 5B) and in situ hybridization (Fig. 5C) showed robust GHS-R antisense mRNA expression in the vagal nodose ganglion of Tg rats, but not of WT rats. There were TH mRNA-expressing cells that also expressed GHS-R antisense mRNA in the vagal nodose ganglion of Tg rats (Fig. 5D). The mRNA expression and protein levels of GHS-R were significantly lower in Tg rats than in WT rats ($P<0.05$) (Fig. 5E).

3.8. The effect of ghrelin on noradrenaline release in BAT

The effect of iv injection of ghrelin on noradrenaline release in BAT was examined. Overall ANOVA demonstrated a significant interaction among genotype, ghrelin injection and time after injection ($F_{8,160}=2.69$, $P<0.01$). Subsequent analysis revealed that ghrelin at a dose of 30 nmol suppressed noradrenaline release in BAT at 20–40 min after iv injection in WT rats (Fig. 6A), but not in Tg rats (Fig. 6B).

4. Discussion

In the present study, the Tg rats had lower body weight and visceral fat weight compared with WT rats on the SD. Furthermore, there was no significant difference in body weight gain between the SD- and HFD-loaded Tg rats, although the total caloric intake on the HFD was significantly larger than that on the SD. In contrast, the HFD significantly increased body weight gain compared with the SD in WT rats. The difference in body weight between WT rats and Tg rats was further confirmed by the difference in visceral fat weight between the two groups; the HFD significantly increased WAT weight compared to the SD in WT rats, while the HFD induced no significant change in the WAT weight of Tg rats. Histological examination revealed that the size of white adipocytes significantly increased and cell numbers per 1 mm^2 of white adipocytes significantly decreased to store more lipids on the HFD compared to the SD in WT rats; these change did not occur in the white adipocytes of Tg rats. These results, together with the higher VO_2 and rectal temperature in Tg rats on the SD, suggest that energy expenditure is elevated in Tg rats compared with that in WT rats, thus causing less WAT mass.

Furthermore, increased dark-phase locomotor activity on the SD and HFD seems to contribute to increased energy expenditure in Tg rats. The increased locomotor activity observed in Tg rats is consistent with the suppressive effect of exogenous ghrelin on locomotor activity [22]. However, the changes in locomotor activity in ghrelin-null mice and GHS-R-null mice are controversial; in one study, ghrelin-null mice showed increased locomotor activity during the dark phase on a HFD [13], while in another study GHS-R-null mice showed decreased locomotor activity during both dark and light phases on a HFD [14]. These differences in locomotor activity phenotypes may come from different impacts of ghrelin knockout, GHS-R knockout, and GHS-R knock down on the regulatory mechanism for locomotor activity and different reactions of its compensatory system.

Although plasma leptin levels were significantly increased by 2-week exposure to the HFD in both WT and Tg rats, the levels were markedly lower in Tg rats than in WT rats on the SD and HFD. In contrast, the serum leptin levels of GHS-R-null mice have been reported to be almost the same as those of WT mice fed with a HFD, and the authors considered that the higher-than-expected leptin levels in GHS-R-null mice may contribute to their hypophagia and increased energy expenditure [14] since leptin suppresses food intake and stimulates energy expenditure through the activation of BAT [23]. However, it is unlikely that the increased energy expenditure is induced by leptin in our Tg rats because of their low leptin levels.

In our previous study [5], we found that GH secretion and plasma IGF-I levels were significantly reduced in female Tg rats but not in male Tg rats. GH increases catecholamine-induced lipolysis in white adipocytes [24,25]. In the present study using male animals, the plasma IGF-I levels of Tg rats again did not significantly differ from those in WT rats on the SD or HFD. Since both male and female Tg rats similarly showed lower body weight and lower WAT in our previous study [5] it seems that reduced ghrelin signal plays a major role to protect Tg rats from accumulation of WAT on both the SD and HFD, and but not GH.

ICV or subcutaneous injection of ghrelin elevates RQ in rodents, indicating an inhibitory effect of ghrelin on fat expenditure as an energy substrate [6]. Therefore, we expected that Tg rats would have a lower RQ in the present study. However, there was no significant difference in RQ between WT and Tg rats either on the SD or HFD. This result may be explained by a decrease in stored WAT mass in Tg rats compared with WT rats, as in another study rats fed only 60% of ad

libitum energy intake for 4 weeks had a reduction in fat mass and increases in RQ during both the light and dark periods [26]. In other words, the RQ in Tg rats might have been elevated by less WAT mass compared with WT rats. This interpretation could be supported by the finding that the stimulatory effect of ghrelin on RQ depends on an increase in food intake [27]. In fact, in the present study, the HFD

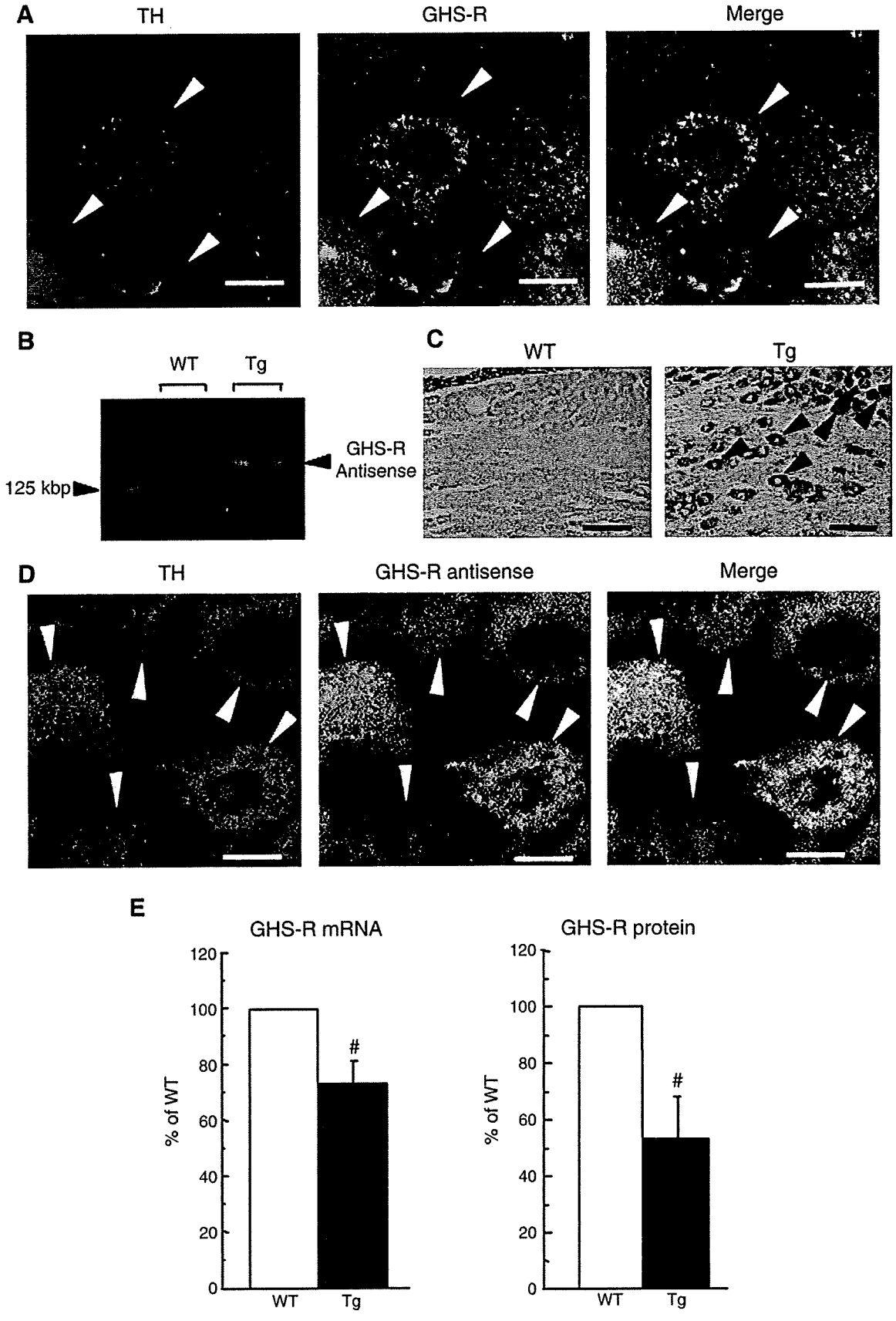

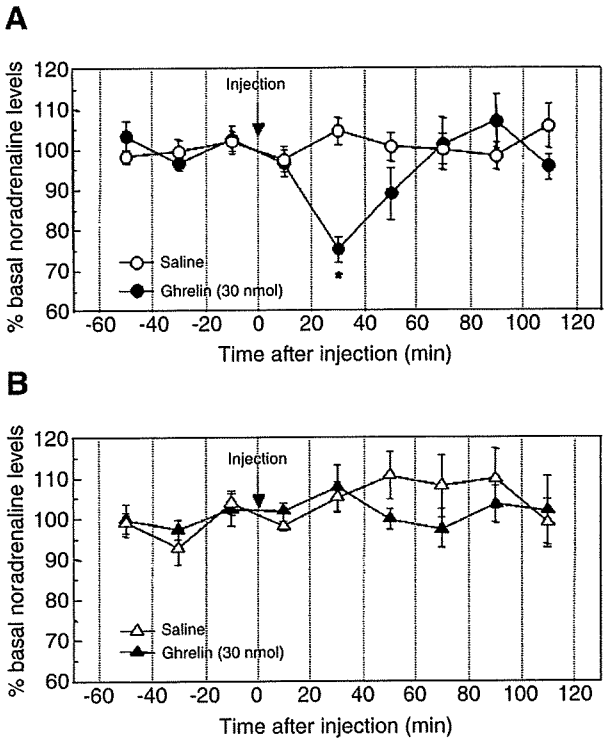

Fig. 6. Effect of iv administration of ghrelin on noradrenaline release in BAT. Ghrelin administration at a dose of 30 nmol significantly suppressed noradrenaline release in the BAT at 20–40 min after injection in WT rats (A), but not in Tg rats (B). Arrows indicate the time of sample injection. Data are shown as mean ± SEM. The number of rats in each group was 7–8. *$P<0.05$, compared with saline-injected WT rats at the same time point.

significantly lowered the RQ in Tg rats whose body weight became almost the same as that of WT rats on the SD. A similar result was reported by another group; they found no difference in RQ between 18-week-old WT mice and ghrelin-null mice that had been fed a SD or HFD in the 3 weeks after weaning [13]. However, the same research group reported significantly lowered RQ in 14- to 16-week-old ghrelin-null mice compared with WT mice after a 6-week exposure to a HFD [11]. Another research group also found significantly lower RQ in 23-week-old GHS-R-null mice compared with WT mice on a HFD for 19 weeks [14]. The Tg rats used in the present study were 10 weeks old and had been fed with the HFD for 2 weeks. Differences in species used for creation of Tg animals, targeted molecules, and methods for treatment with a HFD may explain the different results obtained by different groups.

BAT plays a major role in energy expenditure and non-shivering thermogenesis in rodents. The amount of BAT was significantly larger in Tg rats than in WT rats on the SD and HFD. Histological examination showed that the size of brown adipocytes from WT rats was significantly increased by stored lipid on the HFD. Accumulation of lipid droplets induced a significant increase in the size of brown adipocytes, although BAT weight was not significantly increased in WT on the HFD. The size of brown adipocytes of Tg rats did not significantly change on the HFD. Furthermore, the density of brown adipocytes was significantly lower in WT rats than in Tg rats on the HFD. These results suggest that BAT plays an important role in the resistance to obesity during exposure to HFD; brown adipocytes in Tg rats fully expend the lipid which they take up as an energy substrate, and this expenditure protects them from obesity. In the present study, the higher levels of mRNA expression and protein of UCP1 in Tg rats compared with WT rats indicate that Tg rats have higher activity of brown adipocytes, since the activity level of brown adipocytes is reflected by the expression level of UCP1 protein [28]. It has been suggested that the decrease in ghrelin signaling due to the suppression of GHS-R induces higher expression of UCP1 in BAT of Tg rats, as chronic administration of ghrelin inhibits UCP1 mRNA expression in BAT in a manner independent of ghrelin-induced hyperphagia [27].

Our previous study showed that iv administration of ghrelin inhibits noradrenaline release in BAT in conscious, free-moving normal rats [19]. In the present study, we showed that the inhibitory effect of iv ghrelin on noradrenaline release in BAT is absent in Tg rats. These results suggest that ghrelin inhibits the activity of brown adipocytes by inhibiting the sympathetic nervous system and that the inhibition is not fully driven in Tg rats, thus causing elevated activity of brown adipocytes and decreased WAT mass compared with WT rats. Recently, the stimulatory action of peripherally administered ghrelin on food intake or GH secretion was suggested to be mediated by the afferent vagal nerve, because GHS-R is expressed in 20–40% of cells of the vagal nodose ganglion [16–18] and the stimulatory effects of peripherally administered ghrelin on food intake and GH secretion are attenuated by vagotomy or capsaicin-induced blockade of vagal afferent signaling [17]. Peripheral ghrelin-induced food intake is also abolished by bilateral midbrain transactions rostral to the nucleus solitary tract, which plays a role in mediating the vagal afferent signal to the central nervous system [29]. The present study determined that TH and GHS-R are co-expressed in cells of the vagal nodose ganglion in WT rats. We also found that TH mRNA-positive cells express GHS-R antisense mRNA in the vagal nodose ganglion of Tg rats and that the expression of GHS-R mRNA and protein is significantly reduced in Tg rats. Furthermore, we demonstrated in a previous study that iv administration of ghrelin does not inhibit noradrenaline release in the BAT of vagotomized normal rats [19]. Taken together, these results suggest that the vagal nerve transmits the peripheral ghrelin signal to inhibit BAT activity.

In summary, we analyzed the phenotype of Tg rats expressing antisense GHS-R mRNA under the control of the promoter for TH on a SD or HFD, and found that GHS-R/ghrelin appears to reduce energy expenditure, in addition to stimulation of food intake, by suppressing the sympathetic nervous system innervating BAT and by decreasing locomotor activity. The results also suggest that the GHS-R expressed in the vagal nerve is involved in the signal transduction of peripheral ghrelin to control the function of brown adipocytes.

Acknowledgements

This study was supported in part by Health and Labour Sciences Research Grants from the Ministry of Health, Labour and Welfare of Japan, Grants-in-Aid for Scientific Research from the Ministry of Education, Culture, Sports, Science and Technology of Japan, and a grant from the Foundation for Growth Science. We thank Ms. M. Iketani and Ms. S. Inada for their technical assistance.

Fig. 5. Expressions of TH, GHS-R, and GHS-R-antisense in the vagal nodose ganglion of WT and Tg rats. (A) Immunopositive cells for TH (red, left panel) and GHS-R (green, middle panel) were matched in the merged image (yellow, right panel) in the vagal nodose ganglion of WT rats. Arrowheads indicate co-localization of TH and GHS-R in the same cells. Scale bars, 10 μm. (B) Representative electrophoretic analysis patterns of GHS-R-antisense mRNA in the vagal nodose ganglion of WT and Tg rats. (C) In situ hybridization for GHS-R-antisense mRNA in the vagal nodose ganglion of WT rats (left panel) and Tg rats (right panel). Typical expression of GHS-R antisense is indicated as black arrowheads. Scale bars, 50 μm. (D) Cells expressing TH mRNA (red, left panel) and cells expressing GHS-R-antisense mRNA (green, middle panel) were almost matched in the merged image (yellow, right panel) in the vagal nodose ganglion of Tg rats. Arrowheads indicate co-localization of TH mRNA and GHS-R-antisense in the same cells. Scale bars, 10 μm. (E) The expression levels of GHS-R mRNA (left panel) and GHS-R protein (right panel) in the vagal nodose ganglion were significantly lower in Tg rats than in WT rats. Data are shown as mean percentage of the WT ± SEM. The number of rats in each group was 6. #$P<0.05$.

References

[1] Kojima M, Hosoda H, Date Y, Nakazato M, Matsuo H, Kangawa K. Ghrelin is a growth-hormone-releasing acylated peptide from stomach. Nature 1999;402: 656–60.

[2] Smith RG, Van der Ploeg LHT, Howard AD, Feighner SD, Cheng K, Hickey GJ, Wyvratt Jr MJ, Fisher MH, Nargund RP, Patchett AA. Peptidomimetic regulation of growth hormone secretion. Endocr Rev 1997;18:621–45.

[3] Nakazato M, Murakami N, Date Y, Kojima M, Matsuo H, Kangawa K, Matsukura S. A role for ghrelin in the central regulation of feeding. Nature 2001;409:194–8.

[4] Okada K, Ishii S, Minami S, Sugihara H, Shibasaki T, Wakabayashi I. Intracerebroventricular administration of the growth hormone-releasing peptide KP-102 increases food intake in free-feeding rats. Endocrinology 1996;137:5155–8.

[5] Shuto Y, Shibasaki T, Otagiri A, Kuriyama H, Ohata H, Tamura H, Kamegai J, Sugihara H, Oikawa S, Wakabayashi I. Hypothalamic growth hormone secretagogue receptor regulates growth hormone secretion, feeding, and adiposity. J Clin Invest 2002;109:1429–36.

[6] Tschöp M, Smiley DL, Heiman ML. Ghrelin induces adiposity in rodents. Nature 2000;407:908–13.

[7] Lowell BB, Spiegelman BM. Towards a molecular understanding of adaptive thermogenesis. Nature 2000;404:652–60.

[8] Yasuda T, Masaki T, Kakuma T, Yoshimatsu H. Centrally administered ghrelin suppresses sympathetic nerve activity in brown adipose tissue of rats. Neurosci Lett 2003;349:75–8.

[9] Cannon B, Nedergaard J. Brown adipose tissue: function and physiological significance. Physiol Rev 2004;84:277–359.

[10] Sun Y, Ahmed S, Smith RG. Deletion of ghrelin impairs neither growth nor appetite. Mol Cell Biol 2003;23:7973–81.

[11] Wortley KE, Anderson KD, Garcia K, Murray JD, Malinova L, Liu R, Moncrieffe M, Thabet K, Cox HJ, Yancopoulos GD, Wiegand SJ, Sleeman MW. Genetic deletion of ghrelin does not decrease food intake but influences metabolic fuel preference. Proc Nat Acad Sci USA 2004;101:8227–32.

[12] Sun Y, Wang P, Zheng H, Smith RG. Ghrelin stimulation of growth hormone release and appetite is mediated through the growth hormone secretagogue receptor. Proc Natl Acad Sci USA 2004;101:4679–84.

[13] Wortley KE, del Rincon JP, Murray JD, Garcia K, Iida K, Thorner MO, Sleeman MW. Absence of ghrelin protects against early-onset obesity. J Clin Invest 2005;115: 3573–7.

[14] Zigman JM, Nakano Y, Coppari R, Balthasar N, Marcus JN, Lee CE, Jones JE, Deysher AE, Waxman AR, White RD, Williams TD, Lachey JL, Seeley RJ, Lowell BB, Elmquist JK. Mice lacking ghrelin receptors resist the development of diet-induced obesity. J Clin Invest 2005;115:3564–72.

[15] Mano-Otagiri A, Nemoto T, Sekino A, Yamauchi N, Shuto Y, Sugihara H, Oikawa S, Shibasaki T. Growth hormone-releasing hormone (GHRH) neurons in the arcuate nucleus (Arc) of the hypothalamus are decreased in transgenic rats whose expression of ghrelin receptor is attenuated: evidence that ghrelin receptor is involved in the up-regulation of GHRH expression in the Arc. Endocrinology 2006;147:4093–103.

[16] Burdyga G, Varro A, Dimaline R, Thompson DG, Dockray GJ. Ghrelin receptors in rat and human nodose ganglia: putative role in regulating CB-1 and MCH receptor abundance. Am J Physiol Gastrointest Liver Physiol 2006;290:G1289–97.

[17] Date Y, Murakami N, Toshinai K, Matsukura S, Niijima A, Matsuo H, Kangawa K, Nakazato M. The role of the gastric afferent vagal nerve in ghrelin-induced feeding and growth hormone secretion in rats. Gastroenterology 2002;123:1120–8.

[18] Sakata I, Yamazaki M, Inoue K, Hayashi Y, Kangawa K, Sakai T. Growth hormone secretagogue receptor expression in the cells of the stomach-projected afferent nerve in the rat nodose ganglion. Neurosci Lett 2003;342:183–6.

[19] Mano-Otagiri A, Ohata H, Iwasaki-Sekino A, Nemoto T, Shibasaki T. Ghrelin suppresses noradrenaline release in the brown adipose tissue of rats. J Endocrinol 2009;201:341–9.

[20] Shuto Y, Shibasaki T, Wada K, Parhar I, Kamegai J, Sugihara H, Oikawa S, Wakabayashi I. Generation of polyclonal antiserum against the growth hormone secretagogue receptor (GHS-R): evidence that the GHS-R exists in the hypothalamus, pituitary and stomach of rats. Life Sci 2001;68:991–6.

[21] Yamauchi N, Shibasaki T, Wakabayashi I, Demura H. Brain β-endorphin and other opioids are involved in restraint stress-induced stimulation of the hypothalamic–pituitary–adrenal axis, the sympathetic nervous system, and the adrenal medulla in the rat. Brain Res 1997;777:140–6.

[22] Tang-Christensen M, Vrang N, Ortmann S, Bidlingmaier M, Horvath TL, Tschöp M. Central administration of ghrelin and agouti-related protein (83–132) increases food intake and decreases spontaneous locomotor activity in rats. Endocrinology 2004;145:4645–52.

[23] Shek EW, Scarpace PJ. Resistance to the anorexic and thermogenic effects of centrally administrated leptin in obase aged rats. Regul Pept 2000;92:65–71.

[24] Beauville M, Harent I, Crempes F, Riviere D, Tauber MT, Tauber JP, Garrigues M. Effect of long-term rhGH administration in GH-deficient adults on fat cell epinephrine response. Am J Physiol 1992;263:E467–72.

[25] Yang S, Björntor PP, Liu X, Edén S. Growth hormone treatment of hypophysectomized rats increases catecholamine-induced lipolysis and the number of β-adrenergic receptors in adipocytes: no differences in the effects of growth hormone on different fat depots. Obes Res 1996;4:471–8.

[26] Rising R, Lifshitz F. Energy expenditures & physical activity in rats with chronic suboptimal nutrition. Nutr Metab 2006;3:11–9.

[27] Theander-Carrillo C, Wiedmer P, Cettour-Rose P, Nogueiras R, Perez-Tilve D, Pfluger P, Castaneda TR, Muzzin P, Schürmann A, Szanto I, Tschöp MH, Rohner-Jeanrenaud F. Ghrelin action in the brain controls adipocyte metabolism. J Clin Invest 2006;116:1983–93.

[28] Nicholls DG, Locke RM. Thermogenic mechanisms in brown fat. Physiol Rev 1984;64: 1–64.

[29] Date Y, Shimbara T, Koda S, Toshinai K, Ida Takanori, Murakami N, Miyazato M, Kokame K, Ishizuka Y, Ishida Y, Kageyama H, Shioda S, Kangawa K, Nakazato M. Peripheral ghrelin transmits orexigenic signals through the noradrenergic pathway from the hindbrain to the hypothalamus. Cell Metab 2006;4:1–9.

Atherosclerosis 204 (2009) 590–594

Contents lists available at ScienceDirect

Atherosclerosis

journal homepage: www.elsevier.com/locate/atherosclerosis

Plasma des-acyl ghrelin, but not plasma HMW adiponectin, is a useful cardiometabolic marker for predicting atherosclerosis in elderly hypertensive patients

Yuichiro Yano[a,b,*], Koji Toshinai[c], Takashi Inokuchi[d], Kenji Kangawa[e], Kazuyuki Shimada[b], Kazuomi Kario[b], Masamitsu Nakazato[c]

[a] Division of Internal Medicine, Nango National Health Insurance Hospital, Japan
[b] Division of Cardiovascular Medicine, Department of Medicine, Jichi Medical University School of Medicine, Japan
[c] Division of Neurology, Respirology, Endocrinology and Metabolism, Department of Internal Medicine, Miyazaki Medical College, University of Miyazaki, Japan
[d] Department of Orthopedic Surgery, Kitaura National Health Insurance Hospital, Japan
[e] Department of Biochemistry, National Cardiovascular Center Research Institute, Japan

ARTICLE INFO

Article history:
Received 9 August 2008
Received in revised form
17 September 2008
Accepted 12 October 2008
Available online 1 November 2008

Keywords:
Des-acyl ghrelin
HMW adiponectin
Obesity
Elderly
Atherosclerosis

ABSTRACT

Objective: The coming obesity epidemic in elderly persons necessitates the establishment of new and easy-to-use cardiometabolic markers to identify individuals most likely to develop atherosclerosis among hypertensives.
Methods: We measured plasma HMW adiponectin and des-acyl ghrelin levels, and carotid-artery intima-media thickness (cIMT) in 263 elderly hypertensives (mean 72.6 years; 37%men). Other cardiometabolic markers, including metabolites, inflammation, and hemostasis, were also measured.
Results and conclusion: Both HMW adiponectin and des-acyl ghrelin levels were inversely correlated with obesity. The HMW adiponectin level was favorably associated with glucose and lipid metabolites, PAI-1 (all $P<0.05$), and hs-CRP ($P=0.07$) after adjustment for age, sex, and BMI; however, it had no correlations with cIMT. In contrast, although there were no correlations between des-acyl ghrelin and cardiometabolic markers, except for a positive association with the nitrite/nitrate (NO_x) level ($P=0.002$), des-acyl ghrelin had a significant inverse correlation with cIMT ($P=0.003$). A multivariable regression analysis showed that des-acyl ghrelin, but not HMW adiponectin, was significantly associated with cIMT after adjusting for age, obesity, sex, smoking, 24-h BP, and other cardiometabolic factors ($\beta=-0.178$, $P=0.001$). Moreover, the increased risk of cIMT among those with abdominal obesity compared with non-obesity (0.833 ± 0.185 mm vs. 0.782 ± 0.163 mm, $P=0.019$) was explained by the elevated 24-h BP and reduced des-acyl ghrelin level, but not by other cardiometabolic parameters. These associations were unchanged after adding NO_x to the model. In conclusion, the des-acyl ghrelin level is a useful cardiometabolic marker for predicting atherosclerosis in elderly hypertensives, and the pathologic pathway linking these factors is independent of its NO bioactivity.

1. Introduction

Due to the growing obesity epidemic and the growing elderly population, it is essential that we improve our understanding of the impact of obesity on the cardiovascular system in elderly persons, and establish new and easy-to-use cardiometabolic markers to identify individuals most likely to develop atherosclerosis among hypertensives [1]. A recent study has revealed that endocrine functions (i.e., adipocytokines) are involved in the pathophysiological mechanisms underlying the risk factors associated with obesity and atherosclerosis [2], but the roles of adipocytokines in these mechanisms are only partially understood.

Adiponectin, an adipocyte-derived hormone, has favorable effects on insulin-sensitizing, anti-inflammatory, and anti-atherogenic properties [3], and thus high adiponectin levels have been associated with a reduction of cardiovascular disease (CVD) [3,4]. However, recent prospective studies have shown conflicting results, particularly in elderly persons [5], suggesting that adiponectin may have different clinical implications in the elderly. High adiponectin in the elderly is a consequence of weight loss

* Corresponding author at: Division of Internal Medicine, Nango National Health Insurance Hospital, 1078 Mikado, Nango, Misato Town, Miyazaki 883-0306, Japan. Tel.: +81 982 59 0017; fax: +81 982 59 0213.
E-mail address: yyano@jichi.jp (Y. Yano).

0021-9150/$ – see front matter © 2008 Elsevier Ireland Ltd. All rights reserved.
doi:10.1016/j.atherosclerosis.2008.10.013

and sarcopenia with aging [5–7], both of which are predictors of mortality [8]. In addition, adiponectin could exert its own effects by increasing energy expenditures and thereby leading to wasting [7]. Recently, increasing attention has been paid to the multimeric isoforms of adiponectin. In the circulation, adiponectin exists in at least three multimeric isoforms: a low-, medium- and high-molecular-weight (HMW) form. These different oligomeric forms of adiponectin might activate different signaling pathways and exert distinct functions on its target tissues. Because HMW adiponectin may be the major active form of the metabolic and vascular protective effects of adiponectin [3,6,9], it would be worthwhile to examine its clinical implications in elderly persons.

In contrast, ghrelin, an endogenous ligand for the growth hormone secretagogue receptor (GHSR) and acts as an anabolic hormone in elderly persons [10,11], has been shown to exert not only energy homeostasis, but also cardiometabolic regulations in both healthy and obese subjects [12,13]. The reduction of ghrelin, which is associated with obesity, has also been shown to be proportional to aging and catabolic rates, and thus it may be more representative of a true biological phenomenon in elderly persons. Des-acyl ghrelin, a more abundant form of ghrelin in humans and allows easier measurement than acylated ghrelin, has some unique cardiometabolic properties, such as blood pressure (BP) lowering [12], nitric oxide (NO) production [13], and prevention of cardiac and endothelial cell apoptosis [14]. However, there have been no studies examining these effects in humans.

In the present study, we measured plasma HMW adiponectin and des-acyl ghrelin levels, and examined their relationship to obesity-related cardiometabolic factors, including glucose and lipid metabolism, inflammation (high-sensitivity C-reactive protein: hsCRP), hemostasis (plasminogen activator inhibitor-1: PAI-1), and atherosclerosis (carotid artery intima-media thickness: cIMT) in elderly hypertensives.

2. Subjects and methods

276 consecutive ambulatory patients with essential hypertension who were >40 years old and who had been referred to our outpatient clinic (Kitaura National Health Insurance Hospital, Miyazaki, Japan) were recruited for the Miyazaki Elderly-Fat (EL-FAT) project (see Supplementary materials). The project was approved by the institutional review board at Jichi Medical University, and written informed consent was obtained from all the participants. All patients completed a health questionnaire and provided their complete medical history (smoking and drinking status, physical activity, use of medications, and past medical history), and underwent measurement of body mass index (BMI) and waist circumference (WC), office and 24-h ambulatory BP monitoring (ABPM), blood sampling, and carotid ultrasonography. Hypertension was defined as use of anti-hypertensive drugs or an office BP level of ≥140/90 mmHg. Type 2 diabetes was defined as use of anti-hyperglycemic drugs or a fasting glucose of ≥126 mg/dl. The exclusion criteria were as follows: a history of coronary arterial disease (CAD), cerebrovascular disease, or heart failure in the past 3 months; presence of inflammatory diseases (acute infection, autoimmune diseases); presence of malignant diseases; presence of gastrectomy; and absence of or incomplete sampling data.

2.1. Laboratory testing

To measure the des-acyl ghrelin level, a fasting venous sample was carefully collected via a 21-gauge needle into a syringe containing EDTA-2Na (1.25 mg/ml) and aprotinin (Ohkura Pharmaceutical, Inc., Kyoto, Japan; 500 kallikrein inactivator U/ml) at 08:00–08:30 h. Plasma was obtained by centrifuging the whole blood at 1500 × *g* for 15 min at 4 °C, and was immediately frozen and stored at −40 °C until analysis. We used a commercially available ELISA Kit (Mitsubishi Kagaku Iatron Co., Tokyo, Japan) [15]. HMW adiponectin concentrations were measured using a two-step sandwich ELISA system (FujiRevio Inc., Tokyo, Japan), and the levels of nitrite/nitrate (NO_x) (NO_2^- and NO_3^-) in serum were measured using a high-performance liquid chromatography ultraviolet (HPLC-UV) system. Methods of other parameters are described in detail in the Supplementary materials. The intraassay and interassay coefficients of laboratory tests were all <7%.

2.2. ABPM and carotid ultrasonography

For full details, see the Supplementary materials. Briefly, as described in a previous report [16], cIMT was calculated by averaging the values from three different sites on each common carotid artery: the point of greatest thickness, and points 1 cm upstream and 1 cm downstream from the point of greatest thickness. The average of the right and left cIMT was defined as the mean cIMT.

2.3. Statistical analysis

All statistical analyses were performed with SPSS version 16.0J software (SPSS, Chicago, IL). Data are expressed as the means ± S.D. or median (25th to 75th percentile). The associations between the individual parameters were calculated using Spearman's correlation method. To identify factors associated with the development of cIMT, we used a step-wise multivariable linear regression analysis in which a *P*-value of 0.05 or less in a simple regression analysis was used as the criterion for entry into the model. Variables with skewed distribution were logarithmically transformed before analysis. We also used the κ^2 test for categorical analysis and unpaired *t*-test to compare differences between subjects with or without abdominal obesity, and the difference in cIMT was assessed using ANOVA with post hoc Bonferroni corrections. Statistical significance was defined as $P < 0.05$.

3. Results

3.1. Characteristics of the study population

Two patients who refused to participate, seven patients with incomplete ABPM, and four patients with unsatisfactory blood sampling were excluded. The characteristics of the remaining 263 subjects are shown in Table 1.

3.2. Association of HMW adiponectin with cardiometabolic markers

The plasma HMW adiponectin level was inversely correlated with BMI ($r = -0.215$, $P < 0.001$), WC ($r = -0.253$, $P < 0.001$), ever smoker ($r = -0.203$, $P < 0.001$), GFR ($r = -0.305$, $P < 0.001$), and diabetes ($r = -0.255$, $P < 0.001$), and positively correlated with age ($r = 0.353$, $P < 0.001$) and female gender ($r = 0.185$, $P < 0.001$); however, the significant correlations between HMW adiponectin and BMI and WC disappeared with aging (≥75 years; $n = 118$). The age-, sex-, and BMI-adjusted partial correlations between HMW adiponectin and cardiometabolic markers are shown in Table 2. Additional adjustments for medications, including anti-hypertensive and lipid-lowering drugs, did not alter the associations (data not shown).

Table 1
Characteristics of the study population.

	Total subjects (n = 263)
Age (years)	72.6 ± 8.4
Men, n (%)	96 (37)
BMI (kg/m^2)	24.4 ± 3.5
Waist, cm	86.0 ± 9.5
Ever smoker, n (%)	89 (34)
Anti-hypertensive medications, n (%)	214 (81)
Type 2 diabetes, n (%)	55 (21)
Stain, n (%)	62 (24)
CAD, n (%)	16 (6)
Cerebrovascular diseases, n (%)	25 (10)
GFR	69.6 ± 24.2
ABP measurement	
24-h SBP (mmHg)	134.9 ± 15.4
24-h DBP (mmHg)	77.7 ± 7.8
24-h HR (bpm)	67.2 ± 7.6
Laboratory testing	
Fasting glucose (mg/dl)	99.0 (91.0–112.0)
Insulin (μIU/ml)	5.7 (3.8–8.2)
High-density lipoprotein (mg/dl)	52.0 (44.0–61.0)
Triglycerides (mg/dl)	97.0 (71.0–131.0)
Low-density lipoprotein (mg/dl)	109.0 (91.0–132.0)
hs-CRP (mg/l)	0.58 (0.29–1.09)
PAI-1 (ng/ml)	34.0 (29.0–46.0)
IGF-1 (ng/ml)	103.0 (82.0–130.0)
NO_x (μmol/l)	32.0 (23.0–50.0)
HMW adiponectin (μg/ml)	7.0 (4.2–10.3)
Des-acyl ghrelin (fmol/ml)	108.7 (99.1–159.3)

Data are expressed as means ± S.D. or median (25th to 75th percentile). IGF-1: insulin-like growth factor-1.

3.3. Association of des-acyl ghrelin with cardiometabolic markers

The plasma des-acyl ghrelin level was inversely correlated with BMI (r = −0.155, P = 0.012) and WC (r = −0.162, P = 0.008), but showed no correlation with age, sex, smoking and drinking status, physical activity, or use of any drugs (all P = NS). Intriguingly, stronger inverse correlations between des-acyl ghrelin and BMI (r = −0.256, P = 0.005) and between des-acyl ghrelin and WC (r = −0.323, P < 0.001) were evident with aging (≥75 years). There were no correlations between plasma des-acyl ghrelin and any of the cardiometabolic markers, with the exception of the NO_x level, which showed a positive correlation with the des-acyl ghrelin level (Table 2).

3.4. Determinants of cIMT in elderly hypertensives

Table 3 shows the relation between the cIMT value and patients characteristics, and cardiometabolic markers. In a step-wise multivariate regression analysis including these significant covariates, age, smoking status, 24-h SBP, and the des-acyl ghrelin level remained independently correlated with the cIMT value (Table 4).

Table 2
Age-, sex-, and BMI-adjusted partial correlation among biomarkers.

	HMW adiponectin	Des-acyl ghrelin
Insulin	−0.364 (P < 0.001)	−0.064 (P = 0.301)
High-density lipoprotein	0.191 (P = 0.002)	0.036 (P = 0.560)
Triglycerides	−0.196 (P = 0.002)	0.014 (P = 0.821)
hs-CRP	−0.113 (P = 0.070)	0.076 (P = 0.220)
PAI-1	−0.148 (P = 0.017)	0.041 (P = 0.507)
IGF-1	0.034 (P = 0.585)	0.030 (P = 0.632)
NO_x	−0.009 (P = 0.886)	0.190 (P = 0.002)
HMW adiponectin	–	0.051 (P = 0.415)
Des-acyl ghrelin	0.051 (P = 0.415)	–

Statistical significance was defined as P < 0.05.

Table 3
Univariate analyses with cIMT in elderly hypertensives.

Variable	Spearman's correlation coefficient	P value
Age	0.407	<0.001
Sex (0 = men, 1 = women)	−0.125	0.044
Ever smoker (0 = No, 1 = Yes)	0.150	0.015
BMI	0.051	0.406
Waist	0.109	0.078
24-h SBP	0.259	<0.001
24-h DBP	−0.059	0.340
Insulin	−0.021	0.729
High-density lipoprotein	−0.117	0.059
Low-density lipoprotein	0.060	0.336
GFR	−0.262	<0.001
hs-CRP	−0.046	0.453
PAI-1	−0.122	0.048
IGF-1	−0.110	0.075
NO_x	0.051	0.419
HMW adiponectin	0.122	0.049
Des-acyl ghrelin	−0.180	0.003

Statistical significance was defined as P < 0.05.

Table 4
Multivariate analyses for determination of cIMT in elderly hypertensives.

Variable	Multivariate regression analysis*		
	$\beta^\dagger$	β (95% CI)	P value
Age	0.387	0.004 (0.003–0.005)	<0.001
Sex (0 = men, 1 = women)	0.021	–	0.785
Ever smoker (0 = No, 1 = Yes)	0.184	0.035 (0.015–0.056)	0.001
24-h SBP	0.212	0.001 (0.001–0.002)	<0.001
GFR	0.033	–	0.676
PAI-1	−0.101	–	0.068
HMW adiponectin	−0.010	–	0.863
Des-acyl ghrelin	−0.178	−0.061 (−0.097–−0.025)	0.001

$\beta^\dagger$: standardized coefficient; CI: confidence interval. Statistical significance was defined as P < 0.05.

* Variables with a P-value of 0.05 or less in a simple regression analysis with cIMT were used. Model summary: R^2 = 0.270, P < 0.001.

When NO_x was added to the model, the results were unchanged (data not shown). The significance of these explanatory variables was confirmed by dividing the population into two groups, those with cIMT above or below the median level (see Supplementary materials, Table S1). In addition, receiver–operator curves (ROC) were built to assess the power of biomarkers to predict a high cIMT level. In this way, des-acyl ghrelin was shown to be the best predictor (see Supplementary materials, Figure S1).

3.5. Effects of abdominal obesity and des-acyl ghrelin on atherosclerosis

We divided the subjects into two groups according to the presence of abdominal obesity (defined as WC ≥85 cm in men and ≥90 cm in women) [17]. cIMT was more elevated among those with abdominal obesity than in those without it (Table 5), which difference persisted even after adjustment for sex, smoking, insulin, triglycerides, hs-CRP, PAI-1, and HMW adiponectin (P = 0.022). However, this association was no longer significant after adding 24-h SBP (P = 0.151) or des-acyl ghrelin (P = 0.061) to the model. When added NO_x added to the model, the result was unchanged (data not shown).

4. Discussion

Our data indicate that although reductions of both plasma des-acyl ghrelin and plasma HMW adiponectin are associated with obesity, only the former is a useful cardiometabolic marker for pre-